UNIVERSITY OF OULU

FACULTY OF INFORMATION TECHNOLOGY AND ELECTRICAL ENGINEERING

DEGREE PROGRAMME IN WIRELESS COMMUNICATIONS ENGINEERING

MASTER'S THESIS

LINK LEVEL SIMULATIONS FOR 5G REMOTE AREA SCENARIO

Author	Mohiuddin Mazumder
Supervisor	Docent Harri Saarnisaari
Second Examiner	Dr. (Tech.) Heikki Karvonen

Jun 2021

Mazumder M. (2021) Link Level Simulations for 5G Remote Area Scenario. University of Oulu, Faculty of Information Technology and Electrical Engineering, Degree Programme in Wireless Communications Engineering. Master's Thesis, 54 p.

ABSTRACT

The main object of this thesis is to utilize the Vienna 5G link-level simulator and to introduce modifications which are needed to include new scenarios, such as remote area case. The Vienna 5G link-level simulator is a simulation platform for promoting 5th generation (5G) research and development for the mobile communications system. This work gives a general overview of the link-level simulator platform to evaluate the average performance of the 5G physical layer (PHY) schemes.

In many places across the world, there is no reliable internet connectivity in remote areas. Remote area connectivity is a kind of "missing scenario" of standard 5G solution, which focuses on improved data rate, latency, and massive internet of things (IoT). This work addresses views of connectivity in remote areas with 5G solutions, focusing on wireless radio technologies. The study of 5G physical layer performance evaluation is performed for downlink transmission using single-input and single-output (SISO) techniques. This thesis focused on the performance of waveforms, which can be effectively used in remote area communication systems. The analysis of the simulation results signifies that generalized frequency division multiplexing (GFDM) would be the better option for remote area communication than other waveforms investigated in this study. This work also focused on the performance of channel coding schemes in order to determine the appropriate channel coding scheme for the 5G mobile communication system for medium length message transmission in remote area communication. The polar code appears to be the best possible channel code for medium-length message data transmission in remote areas based on the study of channel coding schemes.

Key words: 5G, Vienna link-level simulator, Waveforms, Channel coding.

TABLE OF CONTENTS

FOREWORD

The motivation of this thesis is to use Vienna 5G link-level simulator to test the link-level simulations for 5G remote area scenarios. This thesis work was performed at the Centre for Wireless Communications (CWC) in association with the 5G RANGE project. During the thesis, it was very pleasing to work with Dr. (Tech.) Heikki Karvonen, a very motivated research person. I'm very grateful for his continuous guidance and support throughout my thesis. The most amazing person I've ever met, to whom I owe special thanks for the great opportunity he has offered me. I'm also very thankful to Docent Harri Saarnisaari for his guidance, advice, and mentorship on various situations, who research in the same field, who was ready to co-evaluate the thesis.

I would like to thank my parents, sister, brother, and my wife, for having faith in me all the time. They have always supported me, and I wouldn't have endured this process without their encouragement. Also, I want to thank all my friends for their support and for making my whole journey beautiful.

Ultimately, I want to acknowledge all those who contributed to this master's thesis analysis explicitly or implicitly.

Oulu, Jun 24, 2021

Mohiuddin Mazumder

LIST OF ABBREVIATIONS AND SYMBOLS

2G	second generation
3GPP	third generation partnership project
4G	fourth generation
5G	fifth generation
ACLR	adjacent channel leakage ratio
AWGN	additive white Gaussian noise
BER	bit error rate
B-DMC	binary-input discrete memoryless channels
BS	base station
BM	base matrices
CRC	cyclic redundancy check
CA-Polar	CRC-aided polar
CP	cyclic prefix
DS	delay spread
DFT	discrete Fourier transform
eMBB	enhanced mobile broadband
EPA	extended pedestrian A
ETSI	European Telecommunications Standards Institute
FSPL	free space path loss
F-OFDM	filtered orthogonal frequency-division multiplexing
FER	frame-error rate
FFT	fast Fourier transform
FEC	forward error correction
GFDM	generalized frequency division multiplexing
GSM	global system for mobile communication
ICT	information and communication technologies
ICI	inter carrier interference
IoT	internet of things
ITU	international telecommunication union
IMT	international mobile telecommunications
LTE	long term evolution
LTE-A	long term evolution advanced
LOS	line-of-sight
LL	link-level
LDPC	low-density parity-check
LLR	log-likelihood ratio
LMMSE	linear minimum mean square error
MAC	medium access control
MAP	maximum a-posteriori
mMTC	massive machine type communications
MF	matched filter
MIMO	multiple input multiple output
ML	maximum likelihood
MM	millimeter
MMSE	minimum mean square error
mm-wave	millimeter wave

NLOS	non-line-of-sight
NR	new radio
OFDM	orthogonal frequency-division multiplexing
OOB	out-of-band
PL	path loss
PAPR	peak-to-average-power ratio
PDP	power delay profile
PHY	physical layer
PSD	power spectral density
QAM	quadrature amplitude modulation
RMS	root mean square
RLC	radio link control
RSC	recursive systematic convolutional
RF	radio frequency
SISO	single-input single-output
SNR	signal-to-noise ratio
SC	successive cancellation
SCL	successive cancellation list
TV	television
UE	user equipment
URLLC	ultra-reliable low latency communications
V2V	vehicle-to-vehicle communication
V2X	vehicle-to-everything communication
WRC	world radio conference
ZF	zero forcing

A	transmitter matrix
B	bandwidth
c	the speed of wave propagation in the medium
C_i	the average power of the relative delay
f_c	the observed frequency
f_D	Doppler frequency
T_p	total power of signal
L	a sequence of bits
n	the sampling index
N	the number of paths
N_{error}	the number of error
N_{bits}	the number of total bits
N_{cp}	the size of the cyclic prefix
N_f	the number of symbols per frame
N_s	the total number of sub-carriers
N_{ch}	the channel impulse response length
N_G	the number samples in the guard interval
N_o	the thermal noise
P_{bits}	the probability of bit error
P	the maximum number of possible paths for propagation
Q	the receiver matrix
k	Boltzmann’s constant

ϑ	temperature
R_p	received power
T_p	the transmission power
T_x	the transmit vector
T_m	the transmitter matrix
T_p^*	the fixed transmission power
d	distance
f	frequency
K	offset
C	capacity
d_s	the data symbols
H	the channel matrix
v	the velocity of the wave relative to the receiver
$v_G(n)$	the received signal
$w(n)$	the additive white Gaussian noise
$z(k)$	the transmitted signal
$z(n)$	time-domain data signal

1 INTRODUCTION

Future generations of mobile communications systems will motive a very wide scope of applications. Each scope has its unique set of specifications in terms of reliability, data rate, user density, and latency [1]. However, the number of mobile traffic is still increasing and the need for higher comprehensive broadband services is further pushing the limits of current standards to further integrate the wired and wireless worlds. The fifth-generation (5G) allows for a new type of network to connect nearly everyone and everything, especially devices, machines, and objects. It has been developed with increased capacity to support next-generation user engagements, allow new deployment patterns, and execution of new services [2].

After the development of 5G standardization, now commercial 5G deployments are taking place across the globe. Third generation partnership project (3GPP)-compliant base stations and applications are now under implementation, based on release 15 specifications [3]. Release 15 provides the context for the implementation of 5G new radio (NR) commercial standard applications, focusing on enhanced mobile broadband [3]. Release 16 introduces new capabilities enhancement and extension to various vertical areas, including unlicensed spectrum support, automotive applications, industrial internet of things (IoT), backhaul, and integrated access support [4].

These advancements will result in a massive growth in mobile and wireless traffic volume, which is expected to expand thousand-fold in the next several years. It's also expected that the current dominating situation of human-centric communication systems will be accompanied by massive growth in the volume of communicating devices. A wide variety of communication features will lead to the coexistence of machine and human-based applications [5].

1.1 Background and motivation

5G mobile technologies are the next generation of mobile communications infrastructure that are developed to upgrade existing mobile networks. 5G technologies have been adopted in response to the growing need for mobile data. 5G networks are intended to handle growing consumer data demand and promote new services. 5G was also developed to fulfil the rising needs for data from industrial customers, as well as to promote the wide use of mobile communications technology in several industries [5].

Nowadays, every telecom company has drawn up the roadmaps for the upcoming 5G mobile networks, which provide higher data speeds and more secure connectivity [6], [7]. 5G just started the transition to a fully connected networked society, which offers access to information and data sharing everywhere and anytime for everyone [8]. Therefore, wireless connectivity is not only a matter of connectivity in the future but of anything that profits from connectivity [9]. The 5G technology is projected to offer enhancement in coverage, mobile traffic efficiency, and additional performance-enhancing technologies through providing increased speeds, reduced latency, ultra-high reliability, and increasing base station densities over each generation. In fact, it is expected that not only the cellular communications for humans but the percentage of machine-to-machine communications increase tremendously. The IoT makes our daily lives more straightforward, more relaxed, and more productive [2].

Based on these scenarios, statistics, and forecasts the approach of society is developing will lead to improvements in the way wireless and mobile communication technologies are utilized. Essential activities such as e-learning, e-banking, e-health, and e-commerce are still growing

and becoming increasingly. On-demand entertainment and information will gradually be supplied via wireless and mobile networks [5].

The objective is to customize a system that provides sustainable rural services through active network deployments and suitable business models. Representative use cases have subsequently been developed, including voice and data connectivity and wireless backhaul, to meet necessary infrastructure and services and other advanced uses, such as smart farming and remote health services [11]. Besides, the network specifications for long-range coverage and non-licensed bands of TV whitespace (TVWS) [13].

Furthermore, the possibility to provide reliable connectivity for remote area users using 5G network. The development of 5G technology offers potential as a way of delivering network services for unconnected rural or remote residents, which is a big business potential given that over half of the population of the world is not accessible to the internet [9]. 5G can be used to support of remote area services for education, entertainment, social media, and several IoT applications. The 5G connectivity in remote areas might have a major impact on lifestyles, opportunities for businesses, and society in general [13].

1.2 Thesis contribution

Flexible connectivity and high data rate transmission capabilities make wireless communication systems increasingly attractive. Despite the huge prospects, these higher data rates and reliable communication are usually not addressed to the remote area [11]. The major aim of this thesis work is to introduce a remote area scenario using the Vienna 5G link-level simulator [12]. This remote area scenario is based on the 5G network for unconnected or underserved remote area users. The scope of the remote area scenario is to provide high-speed internet access in a remote area. In general, the purpose of this work is to evaluate the performance of the physical layer component, such as waveforms and channel coding schemes for remote area communication.

The thesis brings a discussion about an extensive and fair comparison among the sufficient waveform candidates for the remote area communication. This work is to check the viability of the suitable candidate of the waveform for the 5G standard, especially on remote area scenarios. The performance of the different waveforms is evaluated by simulations for remote area communication. This work also evaluates the performance of the channel coding schemes such as low-density parity-check (LDPC) and polar code for the remote area communication based on the additive white Gaussian noise (AWGN) and ‘Pedestrian A’ channel. The performance is reported in terms of bit error rate (BER), frame error rate (FER), power spectral density (PSD), and throughput.

1.3 Outline

This thesis is organized as follows. Chapter 2 consists of the necessary theoretical background of radio access techniques for remote area communications. Also, it introduces the candidates of the 5G waveforms and channel coding schemes. Chapter 3 presents the structure and the functions of the Vienna 5G link-level simulator tools. In addition, it explains the structure of the remote area scenario and its phase-by-phase implementation. Every section handles a functional block such as a transmitter, channel, and receiver. It gives detailed information regarding the choices, simplifications, and assumptions of the remote area scenario used. Chapter 4 introduces the analytical model for performance evaluation of SNR, path loss, BER,

and FER. Chapter 5 investigates the performance of comparing the different channel coding schemes and waveforms in terms of the BER, PSD, and FER. Moreover, the remote area scenario presents several simulation results of the performance between two remote area users. Finally, the simulation results of this thesis are concluded and summarized in Chapters 6 and 7 regarding remote area communications.

2 5G NEW RADIO ACCESS FUNDAMENTALS

Cellular systems have been massively updated from their preliminary stage of analogue communication to include today's high data rate internet capability. The global system for mobile communication (GSM) became the first worldwide standard as the second generation (2G) mobile technology defined by the European Telecommunication Standards Institute (ETSI) [15]. The launch of 5G would require increased data speeds and high capacity in dense installations for the demanding enhanced mobile broadband (eMBB) use case and related new services [15].

The 5G solution is supposed to enhance significantly mobile networking capabilities. There are a number of features that are unique for 5G radio access compared to the previous generations. The foundation of every mobile communication network is wireless technology, which connects the mobile phone to base stations. The 5G wireless access network is supposed to produce ultra-reliability, high data rates, very low latency, low energy usage, and huge heterogeneity [2].

5G's goal is to provide comprehensive coverage for several specific types of services. There are three main challenges to create a fully networked society [16]:

- The need to connect more devices has increased tremendously,
- A significant increase in the volume of traffic and
- A wide range of systems with different characteristics and specifications.

5G NR mobile coverage requires not only different functionalities but also considerably more spectrum and large frequency bands to overcome these challenges.
Figure 1 shows the current (2G, 3G, and 4G) and future (5G) operational frequency ranges of mobile communication systems, where f is indicated as a frequency and λ is the wavelength [16].

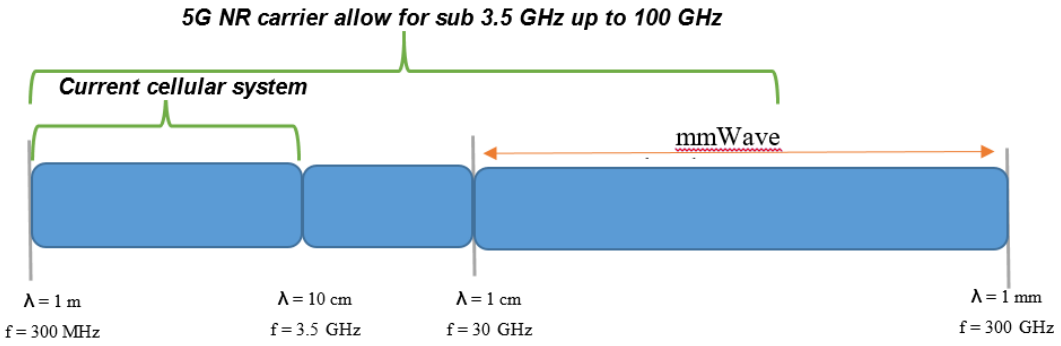

Figure 1. The frequency spectrum for mobile communication systems [16].

The cellular systems currently operate under 3.5 GHz. The mm-wave frequency band (30–300 GHz) offers a large amount of spectrum. 5G NR is planned to operate at frequencies of less than 1 GHz up to 100 GHz. But the mid-band spectrum (1-6 GHz) plays a crucial role in making 5G NR mainstream. The 3.5 GHz (3.5–3.8 GHz) frequency band is nearly worldwide and has been approved in many countries [16]. The vision of the 5G mobile communication frequency spectrum is demonstrated in Figure 2 [16].

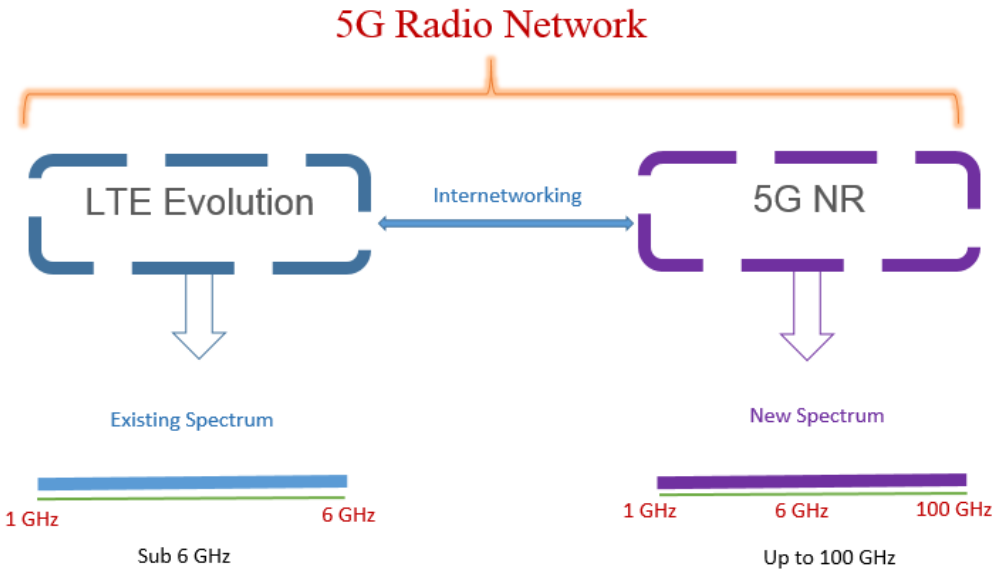

Figure 2. Illustration of 5G radio access vision including evolved LTE and NR [16].

The wireless communication 5G system consists of both the 5G NR and the long term evolution (LTE) enhancements [17]. Close integration between NR and LTE technology is required to integrate NR and LTE traffic effectively [16].

2.1 Development phases of 5G NR

The 5G NR is a worldwide wireless specification based on orthogonal frequency-division multiplexing (OFDM) for the upcoming 5G mobile networks. There are two versions: the non-standalone (NSA) 5G NR and the standalone (SA) 5G NR. Initial 5G NR releases depend on current LTE 4G technology in the NSA phase until the 5G core network matures in the SA phase [18]. Figure 3 shows the two standards-based phase to 5G NR [18].

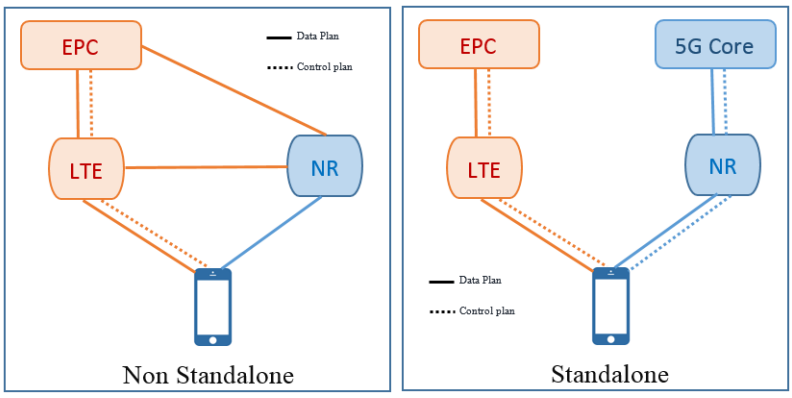

Figure 3. 5G NR development phases [18].

Non-Standalone 5G NR: All industrial 5G applications are now based on a non-standalone NR technology using existing radio access to signals between the network and

devices and developed 5G NSA evolved packet core (EPC) networks that are improved to handle 5G NSA. The non-standalone 5G NR focuses mainly on enhanced mobile broadband (eMBB) to improved data capacity and reliable connectivity but the existing 4G system is used for voice communications [19].

Standalone 5G NR: The standalone (SA) approach for 5G NR networks is a self-contained deployment approach that provides end-to-end 5G coverage. The SA is capable of delivering 5G use cases that demand more than simply high-speed data. A mobile network may achieve ultra-high reliability and ultra-low latencies using SA, which is required for various business-to-business use applications such as self-driving vehicles and industrial plants. As 5G network coverage becomes more widespread, many new use cases for SA will arise [19].

The standalone 5G NR is applied for eMBB, ultra-reliable and low-latency communications (URLLC), and massive machine-type communications (mMTC) to ensure multi-gigabit data rates with increased efficiency and reduced costs [18].

2.2 Spectrum for 5G NR

One of the significant growth factors for the deployment of mobile broadband, fixed wireless networks, and IoT is access to a wide range of spectrum resources. In terms of coverage and capacity, different 5G spectrum frequency bands also offer a range of attributes. Therefore, the availability of a wide range of low-to-mid-to-high-band spectrums are achieved to generate mobile services through a broad range of applications in a large proportion of geographical areas that fulfil public, private, commercial, and consumer demands. In the first releases of NR, 3GPP has been chosen to support the spectrum from below 1 GHz (450 MHz) to 52.6 GHz [16].

To provide broad coverage and assistance for all situations, 5G requires a spectrum across three main frequencies. The three spectrum range are Sub-1 GHz, 1-6 GHz, and above 6 GHz [17]:

- Sub-1 GHz supports broad coverage throughout rural areas, suburban and urban areas and helps support IoT services.
- 1-6 GHz provides a good balance of coverage and performance benefits. The range of 3.3-3.8 GHz forms the base of many initial 5G services. Other frequencies for 5G, including 1800 MHz, 2.3 GHz, and 2.6 GHz may be allocated or reframed.
- Beyond 6 GHz is required to fulfil the ultra-high-speed of 5G. In this range, the 26 GHz or 28 GHz bands currently have the most global recognition.

Accessibility to all three spectrum bands will allow for the full implementation of external and interior coverage, while the entire range of 5G mass-market services is delivered through a stable business model with the optimum socio-economic value.

2.3 5G NR numerology

This section deals with 5G NR frame and sub-frame. The different types of 5G NR slots based on the different subcarrier spacing. The subcarrier spacing of 15, 30, 60, 120, and 240 kHz are supported by 5G NR. The each subcarrier spacing is labled (μ) as a parameter. Here, Δf refers to subcarrier spacing. Table 1 shows the 5G NR transmission numerologies.

Table 1. Supported transmission numerologies [20].

μ	$\Delta f = 2^{\mu} * 15$[kHz]	Cyclic prefix
0	15	Normal
1	30	Normal
2	60	Normal, Extended
3	120	Normal
4	240	Normal

Specifically, 5G Phase 1 introduced different types of subcarrier spacing, as defined in 3GPP TS 38.211 [20]. 4G LTE only supports 15 kHz subcarrier spacing. 5G NR endorsed the normal cyclic prefix (CP) for all the above-mentioned subcarrier spacing options. Unlike LTE, the extended cyclic prefix is only endorsed for μ value of 2 (60 kHz). The subcarrier spacing between 15 kHz to 120 kHz is accessible for data block transmission, like those transmitting user traffic. However, the 240 kHz subcarrier spacing is accessible for synchronization signals [20]. Figure 4 demonstrates a relation of how the cyclic prefix is used [22].

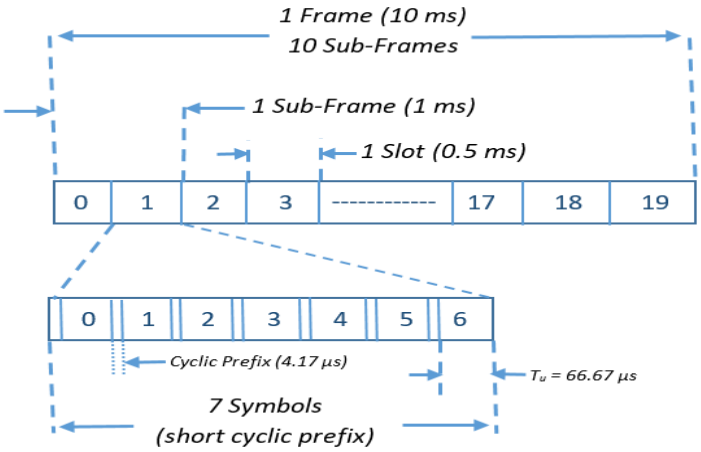

Figure 4. The basic block diagram of cyclic prefix [22].

The slot length is related to the subcarrier spacing Δf and the useful symbol time T_u: $T_u = 1/\Delta f = 66.7\mu s$. Like 4G LTE, 5G NR features a time-domain structure in which transmissions are ordered into 10 ms of frames. Each frame is split into 10 sub-frames of 1 milliseconds each. The each 1 ms sub-frame is split into one or more slots in 5G. The slot length is determined by the value of T_u. Slot length changes according to the different subcarrier spacing [21].

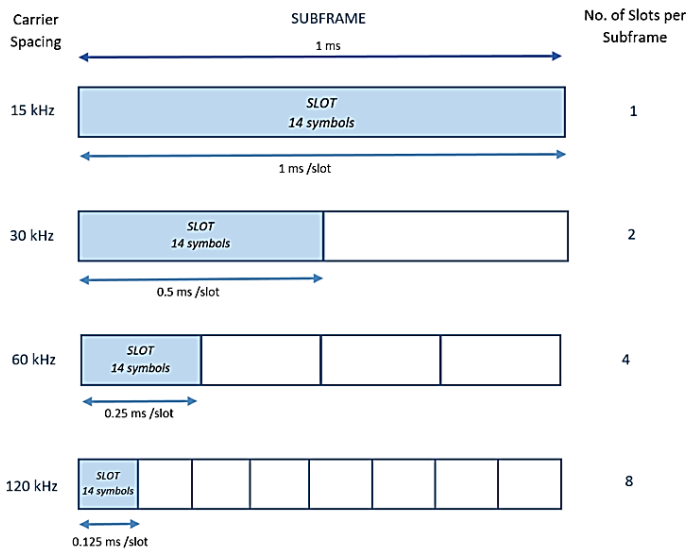

Figure 5. The structure of different slot length [22].

Figure 5 shows the slot length for different subcarrier spacing. 5G NR allows for the various number of slots per sub-frame. Naturally, given that the sub-frame length is 1 ms in any case in 5G NR. The number of sub-frame slots changes depending on carrier spacing. The subcarrier spacing of 15 kHz employs only one slot per sub-frame. The subcarrier spacing of 30 kHz employs two slots per sub-frame and so on. The number of symbols within a slot is 14 [22].

2.4 5G use cases

The goal of 5G mobile communication is to provide integrated connectivity for a range of drastically different types of services and customer needs. The three separate types of services have been listed: eMBB, URLLC, and mMTC. This is well associated with the international telecommunication union (ITU) standards for the mobile communication 2020 and beyond (IMT-2020) [21]. Similar to existing wireless networks, eMBB includes instances of human-centred demand for digital information, applications, and internet connectivity. URLLC is the efficient delivery of packets with stringent specifications, particularly with regard to reliability, latency, and availability. mMTC is distinguished by a significant number of linked devices that usually transmits relatively limited amounts of non-delay-dependent information [16], [21].

The 5G working committee [21] has specified key technological performance and standards for radio interfaces, stating that maximum data rates of 20 Gbit/s for DL and 10 Gbit/s for UL should be achieved. The appropriate spectral efficiencies for these applications are respectively, 30 bps/Hz and 15 bps/Hz. Latency is another important technological condition. For a one-way data transfer, the lowest possible user plane for eMBB is 4 ms, whereas URLLC will require 1 ms. In the case of mMTC, the devices connectivity density of assured quality service quality (QoS) will be at least 10^6 per square kilometre.

2.4.1 Remote area connectivity

In today's information era, having access to advance communications services is becoming increasingly important for sharing in social and economic growth prospects. Accessing and using contemporary communication technologies is particularly difficult for remote populations. Consumers' economic and social well-being are inextricably linked to their ability to use advanced communications services. Since in remote areas, peoples in the globe are one of the economic drawbacks, so it's not unexpected that they have less access to and usage of advanced technologies than the majority of the people. Different countries have implemented a wide range of strategies to focus on enhanced internet access and use in remote areas, ensuring that they do not miss out on the advantages of advanced communications services as well as the welfare-improving possibilities created by online-based delivery of education, health, and a diversity of other services [11], [13].

. The deployment of 5G wireless networks is expected in the near future, according to current telecommunications trends. However, a huge number of individuals do not have access to coverage or internet access. To face this issue, the remote area scenario is focused to investigation 5G applications that access to effective coverage for remote and under-served areas. Consequently, the remote area scenario pursues features that are somehow complimentary to the original IMT2020, for example, long-range coverage, low user density, and lower frequency bands below 1 GHz (700 MHz) [13].

2.4.2 Overview of key use cases in remote areas

In remote area communication, there are useful use cases that can boost local economies and improve the quality of life in underserved regions. The various effective use cases aim to provide connectivity to standard internet services in very wide areas with significant coverage criteria and limited user density. For example, smart farming would create opportunities for regional growth and open new frontiers for productive agriculture. Another possible outcome is that remote health care provides reliable medical assistance for remote areas where there is still a limited or even lacking healthcare infrastructure. Besides, it could theoretically reverse the decline in the population of remote communities by associating these two use cases and even expand new settlements to the farthest regions of the countryside [11], [13]. The multiple strategic key use cases for remote and underserved areas are shown in Figure 6.

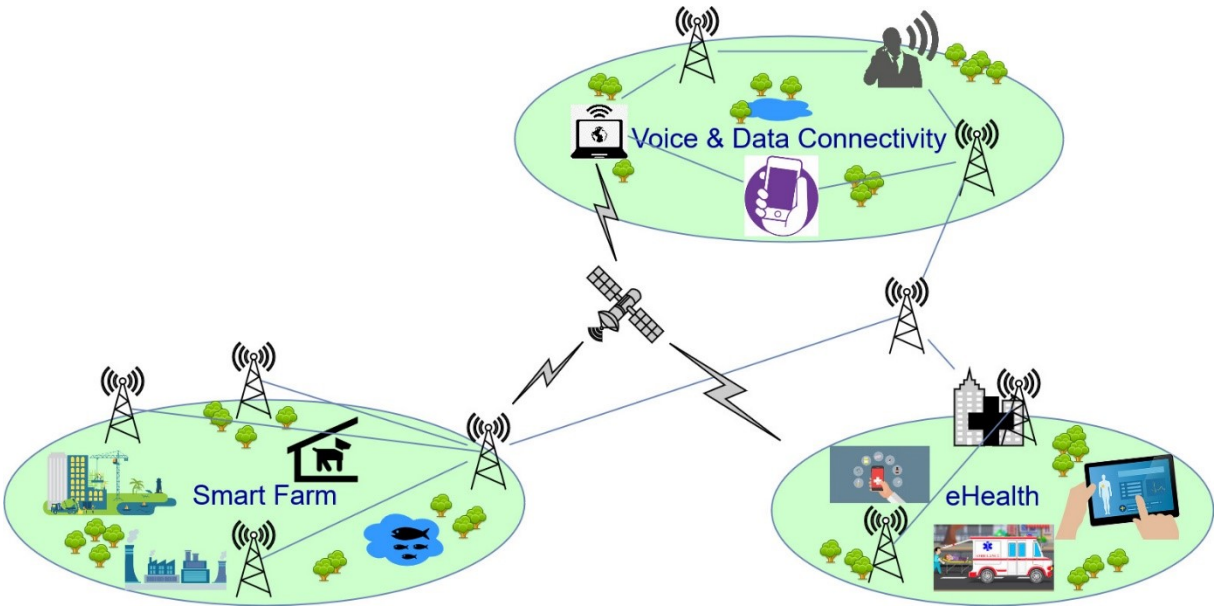

Figure 6. Examples of possible use cases.

The long-distance voice and data connectivity for remote areas use case is targeted at providing long-distance voice and data communication in remote areas. Different services that can be provided with the connectivity of data include improved online access: email, web browsing, file sharing, cloud-based streaming, as well as on-demand digital content [13].

Agriculture and remote area smart farming, in addition to the agro-industrial sector, offers a huge development opportunity for small and mid-size enterprises (SMEs), which leads to changes in almost every agricultural production system. It aims to allow an efficient and cost-effective approach to smart farming. In recent decades, farming has seen many technological changes, which are becoming more industrial and more technologically oriented. Farmers have obtained significant control over the economy of growing livestock and raising crops through the use of different smart farming gadgets, making it more efficient and enhancing their effectiveness. In certain ways, innovations and IoT have the ability to change agriculture. In agriculture, there are several kinds of IoT sensors and applications in general, such as monitoring the accuracy of crops, management of crops, monitoring and management of cattle, and drones for agriculture [23].

Online healthcare for remote areas (e-health) focuses on providing underserved remote areas with health / medical assistance. The e-healthcare environment can provide real-time support by assuming broadband connectivity with sufficient latency. The health monitoring system introduced by IoT for remote areas has an efficient strategy over conventional healthcare. In the healthcare field, various benefits of IoT are seen in the context of wearable and medical applications [23].

2.5 Waveforms

The waveform is an important aspect of any wireless communication system. Waveforms are divided into two categories: single-carrier waveforms and multicarrier waveforms. To transmit data symbols, the single-carrier modulation technique use only one signal frequency [24]. On the other hand, multicarrier modulation systems split the entire frequency channel into many subcarriers, and the high-rate data stream is split into many low-rate data streams that are sent in parallel on the subcarriers [25].

Based on report [14], many waveform candidate physical layer schemes have been considered as possible improvements to the 3GPP LTE-A standard, during the development of 5G NR. NR will support various use cases with different deployments in frequencies. Although single-carrier waveforms can be interesting for massive IoT devices and for operation in high carrier frequencies, the multicarrier waveforms have been seen as main candidates for 5G NR. The 3GPP evaluated several multicarrier waveforms as well as single-carrier waveforms [26]. It was observed that different waveforms have their pros and cons, which makes different waveforms suitable in different scenarios.

The major challenges for the development of the NR waveform include [27]:

- Spectral efficiency,
- Transceiver baseband complexity,
- Multiple-input multiple-output (MIMO) compatibility,
- Low peak-to-average-power-ratio,
- Out-of-band emissions (OOBE),
- Robustness to channel time selectivity,
- Robustness to channel frequency selectivity,
- Synchronization,
- Robustness to phase-noise.

Despite the fact that OFDM is presently the most comprehensive waveform for multicarrier systems, other waveforms for 5G and beyond technology are being studied. It presents intrinsic disadvantages including frequency leak, due to its rectangular pulse shape, the reduction in spectral efficiency due to a cyclic prefix, and the need for fine synchronization of time and frequency in order to maintain the carrier's orthogonality, which ensures low inter-cell interference. Alternative waveforms for 5G and future networks are taken into account. The generalized frequency division multiplexing (GFDM) is one of these waveforms. It is a modulation scheme that employs subcarrier based filtering to reduce out- of-band (OOB) emission [28]. Generally, existing new waveform designs aim to decrease OOB emission leakage and increase spectral efficiency compared to the OFDM technique, which is taken as a reference waveform in most of the waveform studies [27].

2.5.1 OFDM scheme

The OFDM technique is one of the waveform types employed in today's wireless communications systems. The concept of transmitting digital data on several carrier frequencies was utilized in this system, which became a common way for wideband digital communication. It is frequently utilized in wireless communication technology to achieve high data rates and counteract multipath fading. Many wireless networks throughout the

world employs OFDM to achieve high data rates, which are required for data-intensive applications [21]. The OFDM system in terms of the block diagram is presented in Figure 7 [29].

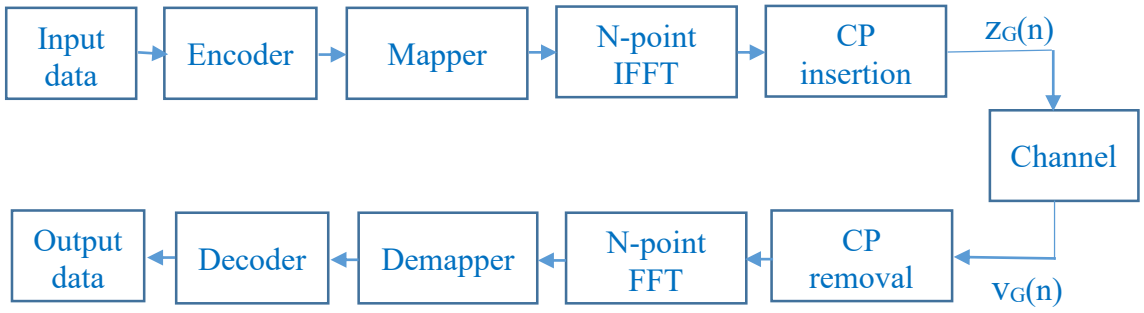

Figure 7. Block diagram of the OFDM [29].

Let $Z_1, Z_2, Z_3, \dots\dots, Z_{N_s}$ be the frequency domain data symbols. The IFFT operation receives these data symbols and processes them. In general, the IFFT carries frequency-domain input information and converts this to the time-domain output information. The respective time-domain data signal $z(n)$ is described below for the k^{th}data symbol [24], [30]:

$$z(n) = \sum_{k=0}^{N_s-1} Z(k)\, e^{j2\pi kn/N_s}, \tag{1}$$

where the total number of sub-carriers is N_s. The CP is assigned by copying the last portion of the IFFT sequence and attaching it to the early part as a guard interval. The length of the CP is calculated based on the channel's maximum excess delay to reduce the impact of inter symbol interference (ISI). The CP can be described as given below [14]:

$$N_{cp} \geq N_{ch} - 1, \tag{2}$$

where N_{ch} is the channel impulse response in samples.

After the CP is inserted, let the time-domain $z(n)$ samples turn into $z_G(n)$ that should pass over the wireless channel. The corresponding transmitted symbol is [25]:

$$z_G(n) = \begin{cases} z(N_s + n)' & n = -N_x, -N_x + 1, \dots\dots, -1 \\ z(n) & n = 0,1, \dots\dots, N_s - 1 \end{cases}, \tag{3}$$

where N_x is the number of samples in the guard interval. Let the resulting received signal expressed as follows [25]:

$$v_G(n) = z_G(n) * y(n,\tau) + w(n) = \int y(n,\tau) z_G(n-\tau) d\tau + w(n), \tag{4}$$

where $y(n,\tau)$ is the fading channel's impulse response, $*$ denotes the convolution between transmitted data symbols and channel impulse response , τ is the delay spread index, and $w(n)$

is the AWGN. The channel impulse response $y(n,\tau)$ consisting of P paths can be described as [25]:

$$h(n,\tau) = \sum_{j=0}^{P-1} y_j e^{j2\pi f_{Dj} t \frac{n}{N_s}} \delta(n-\tau_j) \quad (5)$$

$$= \sum_{j=0}^{P-1} a_n \delta(n-\tau_j), \quad (6)$$

here, P is the maximum number of possible paths for propagation, f_{Dj} is the Doppler frequency shift of the j^{th} path, y_j is the complex impulse response, τ_j is the time delay of the j^{th} path, a_n is the complex path attenuation factor which gives the time-varying complex amplitude, defined as the exponential term [31]

$$a_n = y_j e^{j2\pi f_{Dj} t \frac{n}{N_s}}. \quad (7)$$

The frequency form of this resulting signal will be expressed as follow [25], [31]:

$$V(k) = \left[\frac{1}{N_s} \sum_{n=0}^{N_s-1} v_G(n) e^{\frac{-j2\pi kn}{N_s}}\right]. \quad (8)$$

Ultimately, the signal can be expressed as follows at the receiver end output [25]:

$$V(k) = Z(k)H(k) + W(k), \quad (9)$$

where $Z(k)$ is the transmitted signal in time-domin, $H(k)$ is the channel transfer function represented in the frequency domain, and $W(k)$ is the FFT of Gaussian noise $w(n)$.

2.5.2 GFDM scheme

The GFDM waveform is created by filtering a data block's time and frequency, which provides a flexible, non-orthogonal waveform [32]. GFDM symbol is organized into a block of *MK* samples, where *K* subcarriers bear *M* sub-symbols, allowing the time-frequency layout to be configured to satisfy the specifications for all forms of operation. When filtering the subcarriers, different pulse shaping filters can be used to improve the BER performance and spectral efficiency. A windowing technique can be implemented in the transmitter to further enhance the spectral position [35]. Figure 8 presents the GFDM block diagram of the transceiver [33].

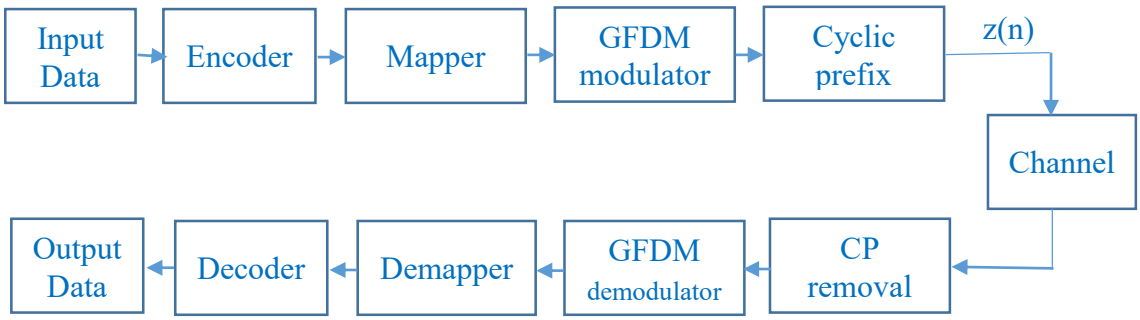

Figure 8. GFDM block diagram [33].

Assume that a GFDM block occupies K subcarriers, each one carrying M sub-symbols, which are temporally equally spaced and cyclically filtered by a prototype filter $g(n)$ with the total number of samples $N = KM$. In discrete-time, the transmitted signal is represented [33],

$$z[n] = \sum_{k=0}^{K} \sum_{m=0}^{M} d_{k.m} \cdot g[(n - mK)_N)] \cdot e^{j2\pi \frac{k}{K} n}, \tag{10}$$

where n is the sampling index, $d_{k.m}$ is the data symbols of the GFDM block on the k subcarriers and m sub-symbols, and $(\cdot)_N$ denotes modulo N operation.

The transmit vector T_x, before the CP addition is described as [34]

$$T_x = T_m d, \tag{11}$$

where T_m is the transmitter matrix with dimensions $KM * KM$, and d is the modulated obtaining the transmitted signal. The transmitted signal T_x is through the wireless channel and can be represented by [34]

$$\mathrm{y(n)} = \mathrm{HT_x} + \mathrm{w(n)}, \tag{12}$$

where H is the band-diagonal structure matrix based on the channel impulse response, and $w(n)$ is the AWGN. The received signal supposing perfect equalization, is expressed as $z = T_m d + w(n)$, then the demodulation is applied to obtain [34]

$$d = Qz, \tag{13}$$

where Q is the receiver matrices, with dimensions $KM \times KM$. The zero forcing (ZF), matched filter (MF), and minimum mean square error (MMSE) are the three most common linear receiver matrices.

The MF equalizer which maximizes the SNR per subcarrier with the impact of introducing self-interference. The MF receiver, which leads to [14], [34]:

$$Q_{MF} = {T_m}^H. \tag{14}$$

where $(.)^H$ is the Hermitian operator. The ZF equalizer that eliminates the self-interference at the effect of enhancing the noise. Standard approaches for GFDM receivers like ZF receiver are already available [14], [34]

$$Q_{ZF} = {T_m}^{-1}. \tag{15}$$

The MMSE equalizer which has a trade-off between the self-interference and noise enhancement. The MMSE receiver jointly execute channel decoding and equalization, minimizing the mean square error of the estimated data symbols. The receiver matrix for this case is given by [14], [34]:

$$Q_{MMSE} = (R_w^2 + T_{m_H} H_{m_H} T_m H_m)^{-1} {T_m}^H {H_m}^H, \tag{16}$$

where R_w^2 represents the covariance matrix of the noise.

2.6 Channel coding schemes

A channel coding scheme is a method that secure the minimum transmission errors in the communication systems. However, among the most important issues with secure digital information transmission over wireless connections is that errors which happen during transmission must often be rectified before decryption can proceed. Channel coding is a process of detecting and correcting bit errors in digital communication systems. Channel coding is performed both at the transmitter and at the receiver. At the transmit side, channel coding is referred to as encoder. Similarly, at the receive side, channel coding is referred to as the decoder [36]. Figure 9 presents the entire channel coding system composed of channel encoder and channel decoder [36].

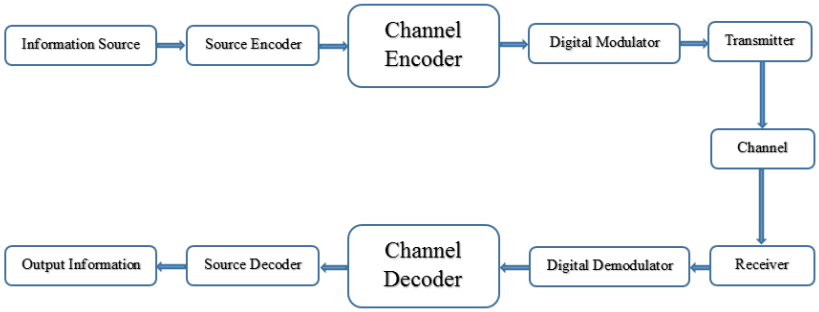

Figure 9. Block diagram of the channel coding scheme [36].

A fundamental digital communication coding scheme consists of the following components: information source, source encoder and decoder, channel encoder and decoder, modulator and demodulator, channel, and information sink. The next subsection presents the polar codes and LDPC code.

2.6.1 Polar code

In 2009, Arikan´s introduced a new type of channel code called polar codes [37], which constructs the first known codes with low-complexity that ideally achieve channel capacity under certain constraints. Polar codes are based on the phenomenon known as channel polarisation, which transforms the transmission channel into digital bit channels with different capacities. Since the polarization level increases to infinite, the input channels become bit

channels that are either totally noiseless or entirely noisy under successive cancellation (SC) decoding. In particular, the technique manages to achieve the symmetric capacity of binary-input discrete memory-less channels (B-DMC), and since the channel is symmetric, the resulting symmetric capacity is equal to the channel capacity [38].

The encoding is basically a linear transformation, whereas the decoding is the approximation of the transmitted information bits based on the received channel values, which is usually expressed as log-likelihood ratios (LLRs). The LLR on the decoder side is measure the probability of a received value corresponding to either 0 or 1 [38].

The SC algorithm is the most common decoding algorithm for the polar codes, which was first proposed by Arikan´s [37]. The polar decoder also used the successive cancellation list (SCL) algorithm [38] and the SCL with cyclic redundancy check (CRC) [40]. The SCL algorithm is an extension of SC. The SCL and SC algorithms work in sequential order. The performance of polar codes can be significantly improved by using an SCL [39].

2.6.2 LDPC code

LDPC code is defined by a sparse parity check matrix. The parity check matrix to be easily adapted to different input lengths. The 5G standard defines two base parity check matrices, or as it is called, base matrices (BM). BM is used depending on the code rate and input size. One BM is more suitable for short lengths and low code rates, while the other is more suitable for long lengths and high code rates [41].

The encoding can be done with low complexity due to the diagonal and dual-diagonal structures of the parity check matrix. The coding is consistent, and a certain number of systemic bits are punctured at the encoder's output [41].

The LDPC decoder is based on layered belief propagation [40] or usually called the sum-product algorithm. The layering is used in the message passage column program. The LDPC decoding algorithms are ‘Min-Sum,’ ‘Sum-Product,’ and ‘PWL-Min-Sum’, where PWL represents for piecewise linear. The LDPC decoder uses linear features to approximate the correction terms similar to the turbo decoder [41].

2.6.3 The channel coding scheme solution chosen for 5G NR

This section addresses the key features of 5G NR channel coding schemes that are specifically intended for the eMBB scenario. An efficient and versatile channel coding scheme is among the NR access technologies' fundamental features required to address higher data rates and additional diverse specifications of standard NR scenarios, along with eMBB, URLLC, and mMTC [43]. In recently published release-15 5G NR cellular technology specifications by 3GPP, two new channel coding techniques of LDPC and polar codes have been proposed to replace the turbo and convolutional codes employed for 4G LTE [27]. In addition, like a 4G system, 5G channel codes might also endorse variable code rates and lengths for both control data and user data. The eMBB scenario, which focuses on reduced latency in 5G cellular communications, uses LDPC coding for user data and polar coding for control information [42].

3 OVERVIEW OF SIMULATION WITH SCENARIO SETUP

This chapter explains the Vienna 5G link-level simulator at the general level. The objective of the Vienna 5G link-level simulator is a thorough analysis of physical layer schemes of existing and future wireless communications systems. The link-level simulator contains multiple waveforms and channel coding methods, which were considered for the 5G communication system. The structure of the Vienna 5G link-level simulator tools for a communication system is composed of three major functional blocks (transmitter, receiver, and channel). Further, some of these functional blocks are divided into smaller functional blocks given in Figure 10.

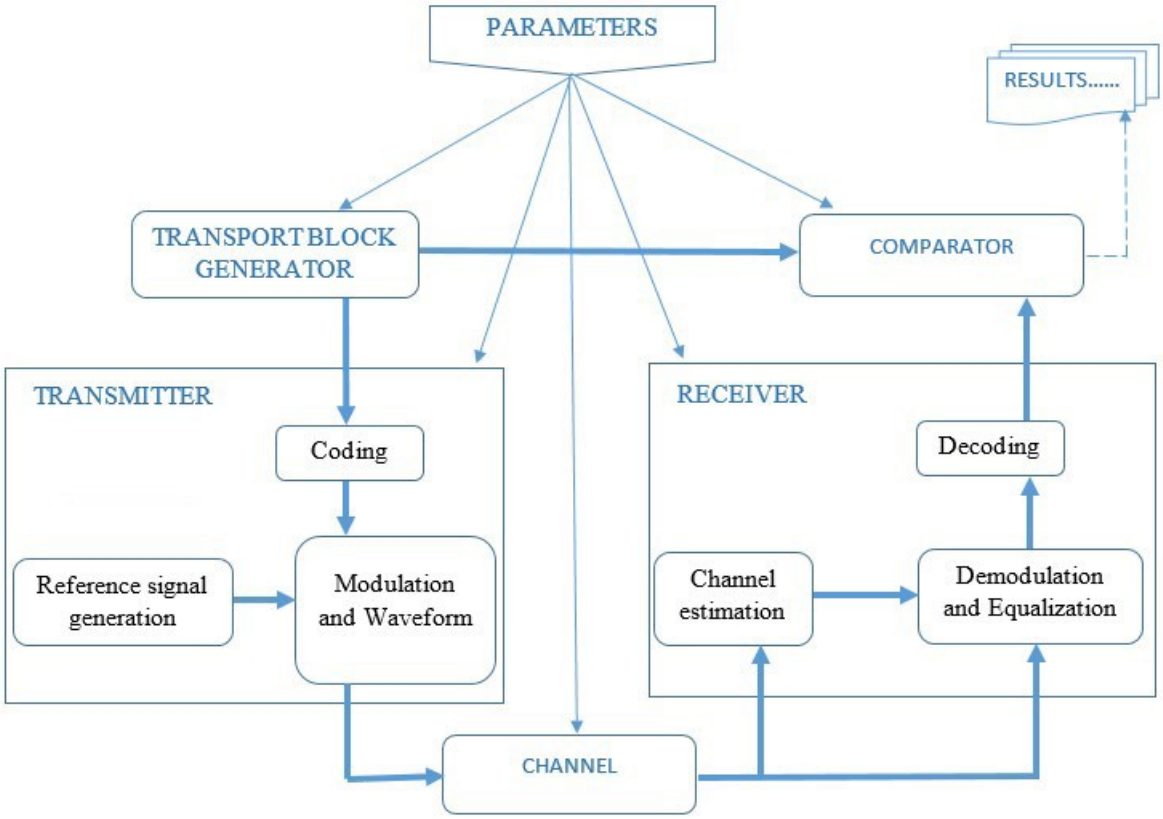

Figure 10. Structure of the Vienna 5G link-level simulation tool.

Figure 10 illustrates the basic processing and simulation steps applied by the simulator. This processing contains the following simulation parameters applied to create a new scenario: carrier frequency, channel coding schemes, modulation and waveform, channel, transmission power, antenna patterns, and large-scale path loss. The 5G link-level simulator supports both uplink and downlink simulations. In this thesis work, only downlink transmission was considered.

3.1 Simulation principles

The Vienna 5G link-level simulator is used to investigate the physical layer performance. The performance evaluation method was mainly concentrated on the effect of channel coding and

waveforms on the PHY layer. The link-level simulator not only supports different waveforms and channel codes in specific, but it also allows us to use different cell to cell parameters. The simulator is simple to use since it allows a wide range of input parameters so that any multicarrier network can essentially be parameterized. The link-level simulator provides pre-defined simulation scenarios in the simulator installation package and allows parameter settings to follow a certain communication standard, like LTE-A or 5G NR. The simulator offers different waveforms, channel coding schemes, single-input single-output (SISO), and supported channel models are based on the power delay profile (PDP) [44].

For interconnection between transmitter and receiver, the link-level simulations assume a defined signal-to-noise ratio (SNR). In the 5G link-level simulator, the path loss of a link is an input parameter, which determines the average SNR for the user. The simulator does not include any spatial network geometry and therefore, the simulator does not introduce any specific path loss model [12]. The objective of link-level simulations is to achieve results with respect to PHY performance metrics, for example, the performance of throughput, the bit error ratio, or the frame error ratio.

3.2 Remote area scenario setup and parameters

The objective of this remote area scenario is to show how different waveforms and channel coding schemes behave under the 50 km distance. The remote area scenario covers the entire transmission chain, along with the specification of the applied channel coding schemes, the multicarrier waveforms, the applied channel model, as well as the equalizers and decoders employed by the receiver.

This section will introduce the input parameters used to investigate the performance of different waveforms and channel coding schemes between BS and UE. The next step is to implement the transmission parameters in the scenario setup. It covers the entire transmission chain, along with the channel coding schemes specification, the multicarrier waveforms, the channel model implemented, as well as the receiver's equalizers and decoders. Chapter 5 provides an overview of the remote area scenario parameters feature of the current 5G link-level simulation tool.

3.2.1 Transmitter

Once the parameters have been specified, the transmitter is built. Three key functional elements are included: topology configuration, coding, and modulation.

3.2.2 Topology configuration

To further explain the specification of topology in different cells, find the topology of the cell network, as shown in Figure 11 [12]. The topology is considered with two cells, and each cell includes one base station. The user one is connected with base station one and thus exists to cell one, while user two is connected with base station two and refers to cell two. Besides that, inter and intra-cell interference can also be easily detected since the corresponding links between the apparently interfering nodes need to be established. In the simulator, each connection is expressed by a link object. Preferred or basic channels appear in solid black,

and interference or secondary channels are presented in red dashed. In addition, each node in a cell using the same number of symbols per frame and subcarriers.

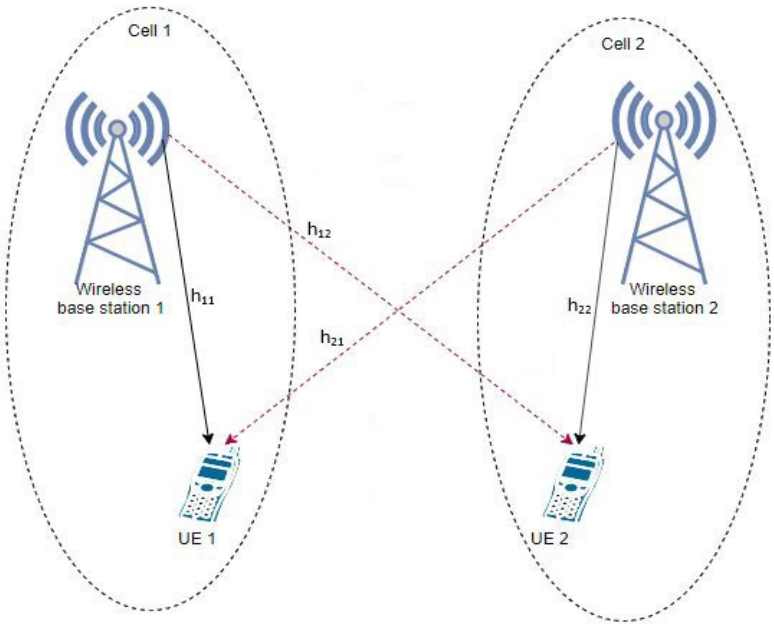

Figure 11. The allocation of user resources within a cell [12].

Code 1. Topology configuration for remote area scenario.

```
scStr.topology.nodes                    = ['BS1,BS2,UE1,UE2'];
scStr.topology.primaryLinks             = ['BS1:UE1,' ...
                                           'BS2:UE2' ...
                                           ];

scStr.topology.interferenceGeneration   = 'Automatic';
scStr.topology.attenuation              = 30;
```

The connections between the nodes are created on the basis of the given 'topology' that essentially tells how nodes are interconnected. To configure the Scenarios.genericScenario.m file from the simulator and modify topology.nodes and topology.primaryLinks. The first feature topology.nodes refer to all of the nodes in the scenario. The next phase is to specify the connected links, once the contributing nodes are entered. The topology.primaryLinks model states that each connection between BS and UE. By defining topology interference generation to 'Automatic,' these interference connections can be programmed automatically, which randomly creates all potential interference relations between the nodes in each cell. By adding attenuation, the strength of interference can be regulated in interference links, where lower attenuation values reflect the stronger inter-cell interference. All users have the same amount of allocated resource elements for a fair comparison. A frequency-domain guard band is used by scheduling between the UE.

3.2.3 Coding

In this thesis, the channel coding schemes (polar and LDPC) are investigated for the remote area communication of the 5G mobile communication standard. The channel coding parameters for the remote area scenario are given in Table 2.

Table 2. The simulation parameters of the channel coding schemes.

Parameter	**Values**	
channel code	LDPC	Polar
decoder	PWL-Min-Sum	CRC-List-SC
list size	32	32
block length	1024 bits	
code rate	1/3	
modulation	BPSK	
channel	AWGN	

This thesis work evaluates the polar and LDPC channel codes for medium-length message transmission in a remote area on an AWGN channel with a code rate of 1/3. The analysis of the different coding schemes is based on the user requirements of the remote area communication. The output results of channel coding schemes are compared in terms of BER and FER.

3.2.4 Modulation waveforms

The 5G link-level simulator specification can contain various modulation schemes for different remote area users. The link-level simulator provides multicarrier waveforms flexibility. According to current 3GPP NR PHY design specifications [27], the standard multicarrier communication scheme in 5G is the OFDM cyclic prefix. Nevertheless, vendors are allowed windowing or filtering above OFDM to lower OOB emissions and increase spectral containment. The remote area scenario investigates the GFDM as a possible waveform for remote area communication. The simulation is used to compare the performance of the GFDM with the OFDM. The simulation parameters of the waveforms are shown for remote area scenarios in Table 3.

Table 3. Waveforms simulation parameter overview.

Parameter	**Value**	
waveform	OFDM	GFDM
filter type/length	-	-
CP length	4.76 µs	4.76 µs
subcarrier spacing	User 1: 15 kHz, User 2: 15 kHz	
guard band	2*15 kHz + 2*15 kHz = 60 kHz	
modulation	64 QAM	
channel model	block fading Pedestrian A	

Code 2. Modulation parameter for remote area scenario.

```
%% Modulation Parameters
% Waveform
scStr.modulation.waveform                   = {'OFDM','GFDM'};

scStr.modulation.prototypeFilter            = 'PHYDYAS-OQAM';

% number of subcarriers per subband
scStr.modulation.nSubcarriersPerSubband     = [12];

% Numerology setup
scStr.modulation.numerOfSubcarriers         = [72,72];
scStr.modulation.subcarrierSpacing          = [15e3,15e3];
scStr.modulation.nSymbolsTotal              = [15,15];
scStr.modulation.nGuardSymbols              = [1,1];
scStr.modulation.samplingRate               = 'Automatic';
```

For remote area scenarios, the number of subcarriers and subcarrier spacing in both cells is the same. Two different cells employ the number of subcarriers, 72 subcarriers for cell one and 72 subcarriers for cell two. Similarly, the same number of subcarrier spacing of 15 kHz is applied for both cells. The both cells employ the same number of symbols per frame. Moreover, the sampling rate is the same for all nodes and is a standard parameter.

3.3 Channel model for remote area

Channel models define the connection characteristics of the transmitter to the receiver. Scattering, absorption, reflection, refraction, and fading are standard features of long-distance communication [46]. The channel is applied and implemented for remote area scenario with the following parameters:

- Velocity = 40 km/h,
- Power delay profile = ‘Pedestrian A’ or ‘Vehicular A’,
- Doppler model = Jakes,
- Carrier frequency = 700 MHz,
- Number of paths for the process = 50,
- Number of transmit antennas = 1,
- Number of receive antennas = 1.

Since the objective of the link-level simulation is to attain the average link efficiency, several random channel realizations are needed per scenario. Therefore, the channel model contains only small scale fading effects, whereas its mean power is determined by the path loss [12].

The channel model based on the power delay profile 'Pedestrian A' is presented for remote area communication. In this remote area scenario, channels keep the same value of attenuation during the whole sub-frame.

3.3.1 Small scale channel model

The frequency selective fading models include the input of the power delay profile for a function. PDP is provided as a vector in this fading model for providing impulses with time delays. The power delay profile interpolated with several potential tap lengths of the filter [27].

The 3GPP TR 38.901 introduces the many channel models for 5G communication in different environments [45]. The objective of the link-level simulation is to obtain the average link capacity. There are also several models throughout the literature for the path loss models that are applicable to a frequency range of 700 MHz and 50 km distance.

Code 3. General transmission parameters.

```
% Set link types to simulate
scStr.simulation.simulateDownlink           = true;
scStr.simulation.simulateUplink             = false;
scStr.simulation.simulateD2D                = false;
% Plot options
scStr.simulation.plotResultsFor             = [1];
scStr.simulation.plotOverSNR                = true;
scStr.simulation.saveData                   = false;
% Define a sweep parameter
scStr.simulation.sweepParam                 = {'simulation.pathloss'};
scStr.simulation.sweepValue                 = linspace(153,75,10);
scStr.simulation.applySweepingTo            = [1];
% Number of simulation frames
scStr.simulation.nFrames                    = 1000;

%% Physical Transmission Parameters
scStr.simulation.centerFrequency            = 7e8;
scStr.simulation.txPowerBaseStation         = [53];
scStr.simulation.txPowerUser                = [53,53];
scStr.simulation.nAntennasBaseStation       = [2];
scStr.simulation.nAntennasUser              = [1];
scStr.simulation.userVelocity               = [40];
scStr.simulation.pathloss                   = [153];
% Nonlinearity model
scStr.simulation.downlinkNonlinearity       = false;
scStr.simulation.amplifierOBO               = [1];
scStr.simulation.smoothnessFactor           = [3];
```

In the design of cellular networks, propagation path loss models play a significant role in defining major system parameters such as frequency, transmission power, antenna parameters, and so on. A path loss is an input parameter that determines the average SNR of the user. The

path loss value is entered in the simulation path loss. This value is 153 dB for free space path loss over 50 km distance.

3.3.2 Pedestrian A

'Pedestrian A' is a channel model that is widely used. This channel model is specified in the ITU-R recommendation [47]. Letter 'A' refers to the delay spreads. The 'Pedestrian A' channel model applied the area for both indoor and outdoor users. The channel´s multi-path delay profile is shown in results section.

Code 4. Channel parameters.

```
scStr.channel.dopplerModel                  = 'Discrete-Jakes';
scStr.channel.timeCorrelation               = false;
scStr.channel.spatialCorrelation            = 'none';
scStr.channel.nPaths                        = 50;
scStr.channel.powerDelayProfile             = 'PedestrianA';
```

The fading taps to match a certain Doppler spectrum in order to the time selectivity of the channel model. A Jakes ' model and a standardized spectrum of Doppler are currently being introduced in this remote area scenario.

3.4 Receiver

The most important feature blocks in the receiver end are channel estimation, equalization, demodulation, and decoding. A more comprehensive system of the receiver is describing next.

3.4.1 Channel estimation and equalization

In advanced LTE and 5G system receivers, the channel estimate is one of the most important phases. The fundamental goal of channel estimate is to figure out the channel response. When a transmission signal travels via a channel, channel estimation offers information on the signal's distortion. Equalizers employ this information to reduce the effect of fading and channel interference, allowing the original broadcast signal to be recovered. The approach of channel estimate technique is used to the estimation frequency domain [48].

Code 5. Channel estimation and equalization parameters.

```
scStr.simulation.channelEstimationMethod    = 'Approximate-Perfect';
scStr.simulation.noisePowerEstimation       = false;
scStr.simulation.pilotPattern               = 'LTE Downlink';
scStr.simulation.equalizerType              = 'One-Tap';
scStr.simulation.receiverTypeMIMO           = 'ZF';
```

Equalization is the reversing of distortion that occurs as a signal travels across a channel. In the Vienna 5G link-level simulator implemented the one-tap equalizer for all waveforms. The equalization is used in order to recover the send data symbols.

3.4.2 Decoding

The channel encoder in the transmitter converts the input bit sequence into a channel input bit sequence, while the channel decoder in the receiver repeats the process. The redundancy in the channel decoder is used to aid in the identification and repair of bit errors, allowing the original transmitted input bit sequence to be determined [38].

Code 6. Channel coding parameters.

```
scStr.coding.code                          = {'Polar', 'LDPC'};

scStr.coding.decoding                      = { 'CRC-List-SC',...
                                               'PWL-Min-Sum'};

scStr.coding.decodingIterations            = [8, 8];
```

In this simulation tool, the Min-Sum-Product decoder algorithm with the number of iterations ($I = 8$) was considered for the decoder components of LDPC code [12]. In this remote area scenario used CRC-list-SC decoding for polar code of code rate 1/3, which has a commonly used SCL decoder for polar code CRC-aided.

4 ANALYTICAL MODEL

An analytical equations are introduced here to calculate the path loss, SNR, BER, FER and throughput of remote area communication performances.

In this work, a free space path loss model was considered. The path loss equation is specify as [14]

$$PL[dB] = 10log_{10}\left(\frac{4\pi df}{c}\right)^2, \tag{17}$$

here f is the frequency in MHz in the free space path loss (FSPL) model, the d is the distance in kilometres.

The SNR is specified as the ratio of signal power to the noise level. For each node, the total transmission power value is set and referred to as T_p, this power is spend equally on the whole scheduled transmission bandwidth B.

The total power of the signal is then provided [12]

$$T_p = \frac{1}{N_f T}\int_{-\infty}^{\infty} P\{|x(t)|^2\}dt\ , \tag{18}$$

where the mean signal power is $P\{|x(t)|^2\}$. Here, N_f refers to the number of symbols per frame, and T refers to the symbols duration.

The SNR is specified as the relation between the thermal noise PSD N_0 and signal PSD T_p/B, which yields [12]

$$SNR\ (d) = \frac{R_p(d)}{N_0 B}. \tag{19}$$

N_0 is constant over frequency band. It comes from

$$N_0 = k\vartheta\ , \tag{20}$$

with the Boltzmann's constant k and temperature ϑ.

In this context, the R_p received power is [12]

$$R_p(d) = T_p^* - PL(d), \tag{21}$$

where the fixed transmission power is T_p^* and PL denotes the path loss. The path loss PL is defined in equation (17).

The SNR is usually expressed in decibels given by the formula

$$SNR\ (d) = 10\log_{10}\left\{\frac{R_p(d)}{N_0 B}\right\}. \tag{22}$$

The BER is calculated the performance of a transmission system can be written as [49]

$$BER = \frac{N_{error}}{N_{bits}}, \tag{23}$$

where the number of errors is N_{error} and N_{bits} is the number of total bits.

The FER is calculated of a transmission system can be written as [50]

$$FER = 1 - (1 - BER)^{L}, \tag{24}$$

where L is the number of bits in the packet.

5 LINK LEVEL SIMULATION RESULTS

This section includes all the outcomes and their corresponding evaluation acquired using the Vienna 5G link-level simulator. Firstly, this work provides a comparison between the channel coding schemes: polar and LDPC codes for medium block length with code rate 1/3, where used the simulator file (comparison_codingschemes.m) from the Vienna 5G link-level simulator. Another object of this work is to examine the OOB emission and error efficiency of the different waveform outcomes through comparison with those of OFDM using the simulator file (comparison_waveforms.m). Finally, this thesis evaluated the two remote area user's throughput performance results using remote area scenarios for 16QAM and 64QAM techniques.

In this chapter, the analysis of some preliminary simulation results is presented to compare waveforms and channel coding schemes performance. The comparisons of the results using the simulation parameters, which are summarized in Table 4.

Table 4. Summary of simulation parameters.

Parameter	**Values**
General	
carrier frequency	700 MHz
subcarrier spacing	15 kHz (UE2) & 15 kHz (UE1)
number of subcarriers	72 (UE2),72 (UE1)
FFT size	1024
type of cyclic prefix	144 samples
no. of symbols for control	2
tx power	UE1:53 dBm & UE2:53 dBm
users	2
Path loss	153 dB (50 km distance)
antenna scheme	SISO
transport format	
transport block size	1024
channel code	Polar, LDPC
waveform	OFDM, GFDM
modulation scheme	BPSK, 16QAM, 64QAM
Channel	
channel type	Rayleigh fading, AWGN
Doppler model	Jakes
power delay profile	Pedestrian A
control channel	error free
Receiver	
channel estimation method	approximate-perfect
equalizer type	One-Tap
decoding algorithm	CRC-List-Sc
number of iterations	8

5.1 Channel coding comparison

The simulation results compares the efficiency of the different coding techniques through Vienna 5G link-level simulation in this subsection. This work is focused only for polar code and LDPC code. Here coding schemes illustrates how iterations (polar and LDPC) influence the performance. PWL-Min-Sum and CRC List-SC are the decoding schemes used for LDPC and polar codes. For a block length of 1024 frames and a code rate of 1/3, this work evaluates the performance of LDPC and polar codes over the AWGN channel with BPSK modulation. Figure 12 and Figure 13 demonstrates the channel coding scheme simulation's BER and FER performance.

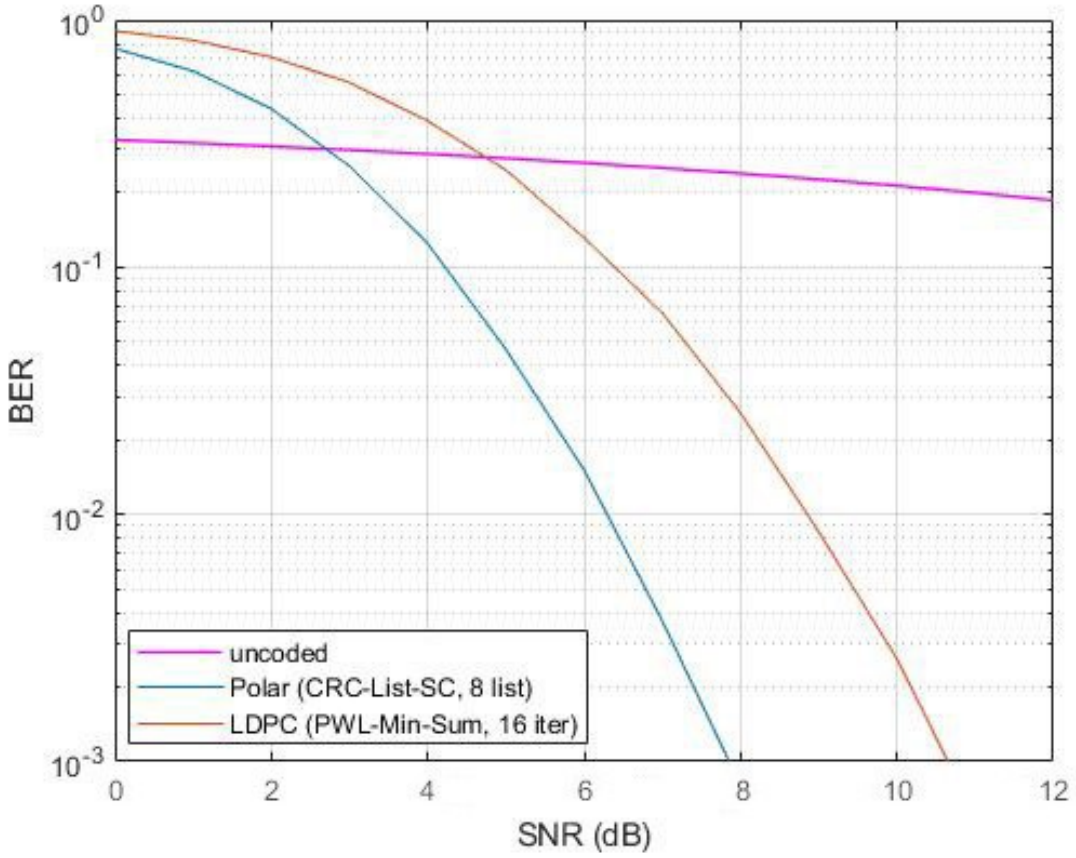

Figure 12. BER vs. SNR performance curve for different channel coding schemes with code block length for 1024 bits.

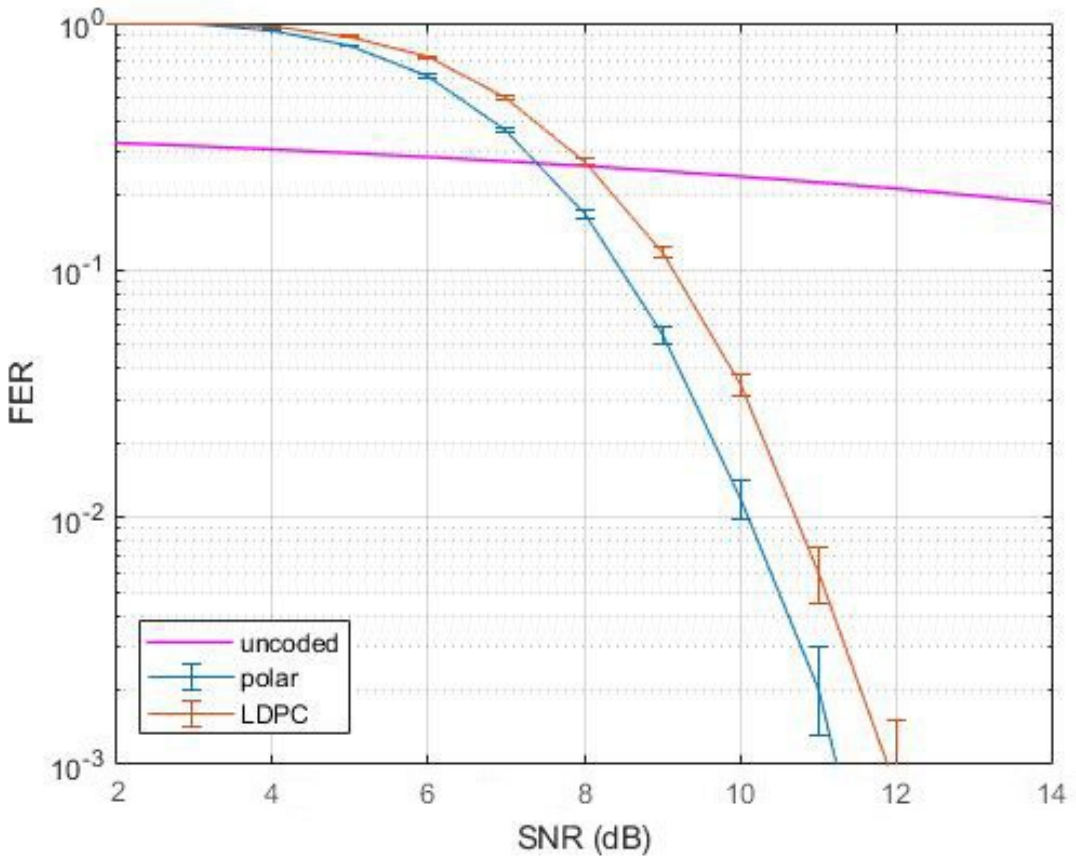

Figure 13. The FER performance for medium block lengths for 1024 bits.

It can be seen that in such a configuration, the polar code has the lowest error probability for BER and FER cases. Figure 12 shows that the polar code is more reliable with a difference of 2 dB compared to the LDPC code at medium block length. It also illustrates that the BER performance of LDPC code is not reliable compare to polar coding schemes for low SNR value. In other words, the polar code shows better performance against the LDPC code at the 10^{-3} FER. The LDPC code also achieves the 10^{-3} FER for high SNR compare with polar code. The summary of the reliability of channel coding techniques for the 5G cellular communication system for medium-length message transmission illustrates that polar code achieves more reliability than LDPC code.

5.2 Channel delay profile

The 5G link-level simulation introduced the 3GPP 'Pedestrian A' channel model as channel delay profile. The 'Pedestrian A' channel model parameters are introduced in Table 5. In a standard PDP model, each multi-path signal power is calculated against its corresponding distances in propagation. A sample power delay profile is shown in Figure 14.

Table 5. ‘Pedestrian A’ channel model [47].

Pedestrian A		
Tap	**Relative delay (ns)**	**Average power (dB)**
1	0	0
2	110	-9.7
3	190	-19.2
4	410	-22.8
5	-	0
6	-	-

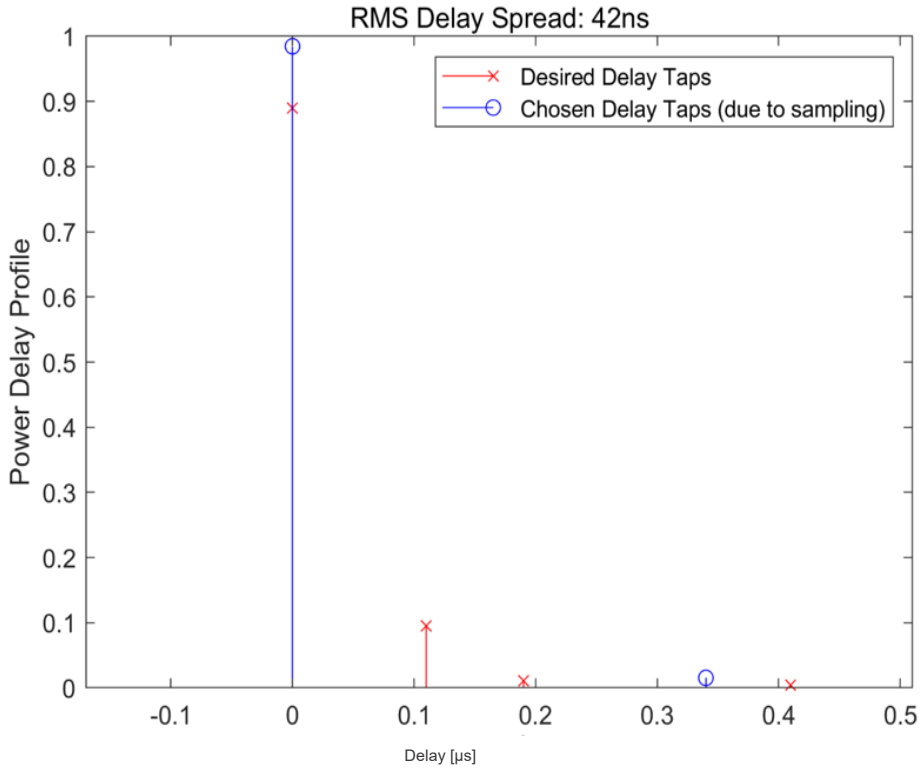

Figure 14. 3GPP ‘Pedestrian A’ channel tapped-delay lines.

The average powers and relative delays for the taps of multi-path channels based on 3GPP recommendation are given in Table 5. The projected value for the 3GPP ‘Pedestrian A’ is defined as the average power at the channel output according to the delay.

5.3 Waveforms comparison

In chapter 2, 5G candidate waveforms have been introduced, and their main block diagram have been described. In this section, the waveforms are compared based on a number of

factors, including their power spectral density and BER performance. The input parameters used to achieve the outcomes are as follows:

- Monte Carlo repetitions: 500
- Sampling rate: $294*10^4$samples/s
- GFDM:
  - Number of sub-carriers: 24
  - Number of sub-symbols: 15
  - Sub-carrier spacing: 15 kHz
  - Cyclic prefix length: $1/(8*GFDM_{SubcarrierSpacing})$
  - Cyclic suffix length: $GFDM_{CP\ Length}$
  - Transmitter pulse: Root-raised cosine
  - Roll-off factor transmitter pulse: 0.1
  - Receiver pulse: Zero Forcing
  - Length ramp smoothing filter: $0.25 * GFDM_{CP\ Length}$
- OFDM
  - Number of sub-carriers: 24
  - Number of sub-symbols: 14
  - Sub-carrier spacing: 15 kHz
  - Cyclic prefix length: $1/(14*OFDM_{SubcarrierSpacing})$

5.3.1 Power spectral density performance

Here, the power spectral density performance is addressed for different waveforms. Number of subcarriers, subcarrier spacing and cyclic-prefix length is chosen from the possible choices specified in the 5G standard. Figure 15 presents the PSD including OOB emission output of OFDM and GFDM waveforms.

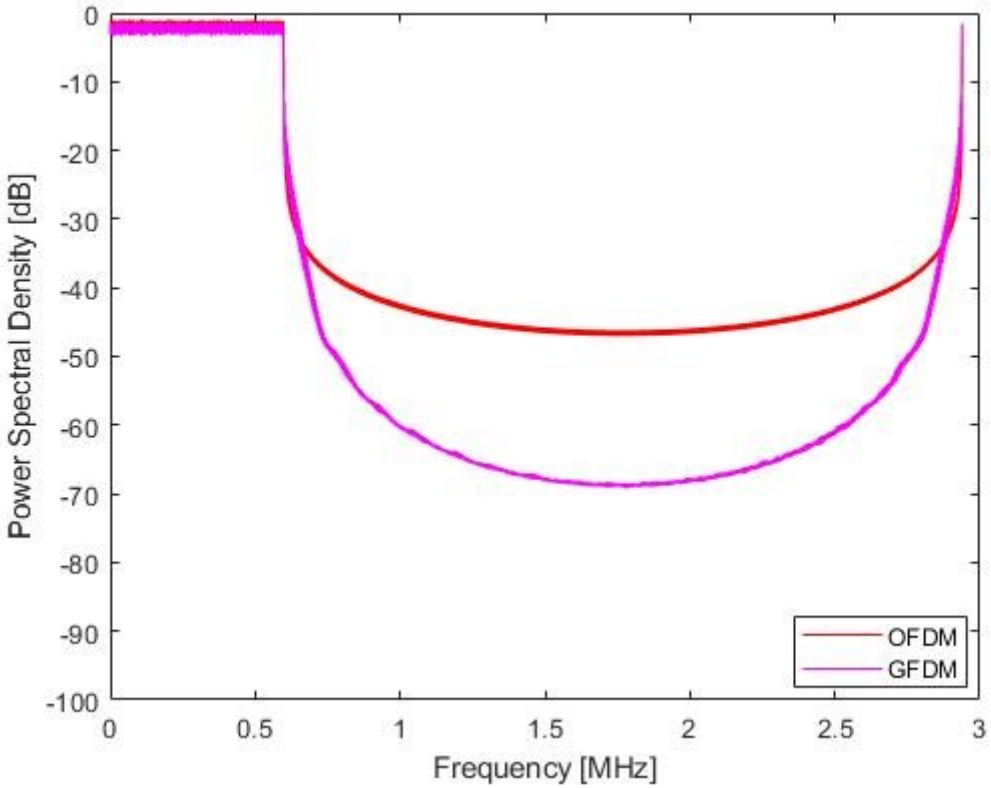

Figure 15. PSD comparison between waveforms.

The comparison between different waveforms related to PSD is shown in Figure 15, where the PSD is indicated in dB as the function of the frequency in MHz. The result illustrates that the OOB power in GFDM is very low compared to the power in the desired transmission band. It is evident that GFDM has better PSD than OFDM in this regard. According to the 3GPP standard, the requirement of OOB emissions of OFDM does not balance with adjacent channel leakage ratio (ACLR) -55 dBc. The power spectral density of GFDM is less, this shows GFDM provides lower spectral efficiency on the side lobes. The OOB emissions can be reduced by selecting the appropriate pulse shaping filter. To note that GFDM waveforms have been able to meet the ACLR requirement for OOB emission.

5.3.2 BER performance

The BER performance of various waveforms is calculated. Here, only one transmitter and the receiver use the full data transmission bandwidth, and there are no interferers in neighbouring frequency bands. The BER performance evaluates using a one-tap equalizer to analyse the performance of waveforms in selective frequency channels. Figure 16 compares the BER performance of OFDM and GFDM waveforms.

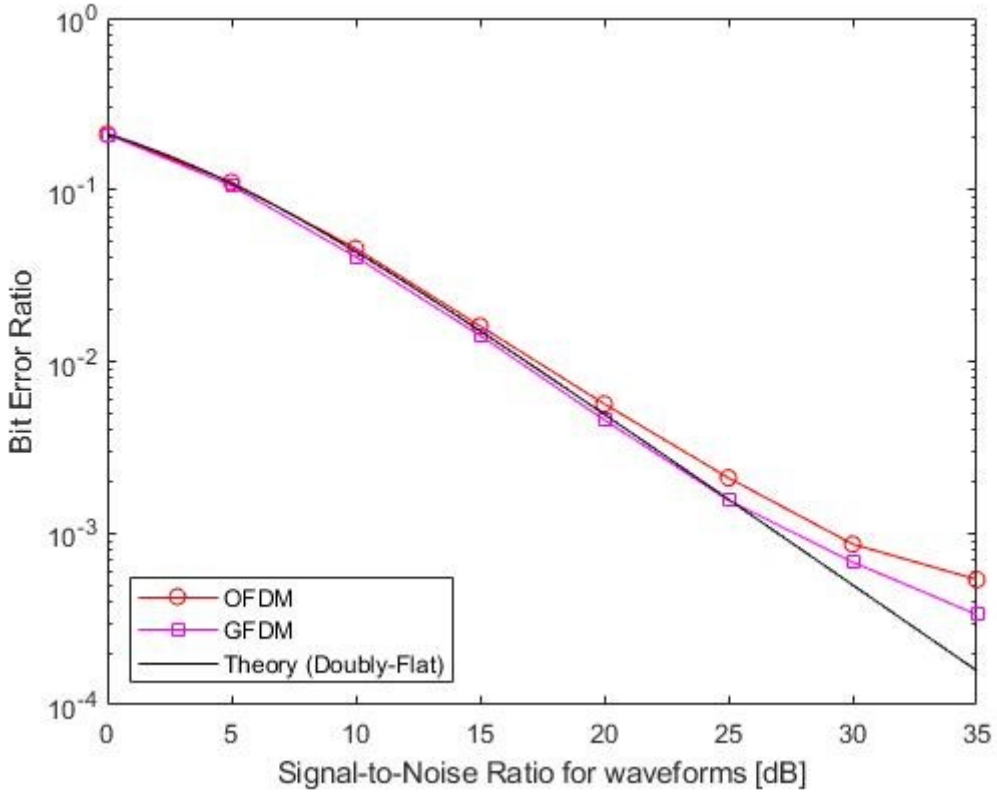

Figure 16. BER of different waveforms for the doubly-selective channel using a one-tap equalizer for 'Pedestrian A' power delay profile.

The results of the BER are estimated using a one-tap equalizer for OFDM and GFDM waveforms performed in the simulator. In terms of bit error rate, the GFDM waveform provides the better error performance at the SNR = 30 dB, as the BER = 10^{-3} is achieved. The behaviour of the OFDM is different. The OFDM system shows slight different error performance in comparison to GFDM waveform based on 'Pedestrian A' power delay profile. At low SNR, the both waveforms performance is close to the theoretical BER that can be achieved with QAM transmission without self-interference. The GFDM waveform has slight better reliability with an advantage of error performance compared to OFDM at high SNR level.

5.4 Path loss

In wireless communications, the distance between the transmitter and receiver tremendously affects the quality of the communication signal. Figure 17 shows the path loss versus distance curve for different distance values. Path loss can be calculated using Equation (17) of Chapter 4.

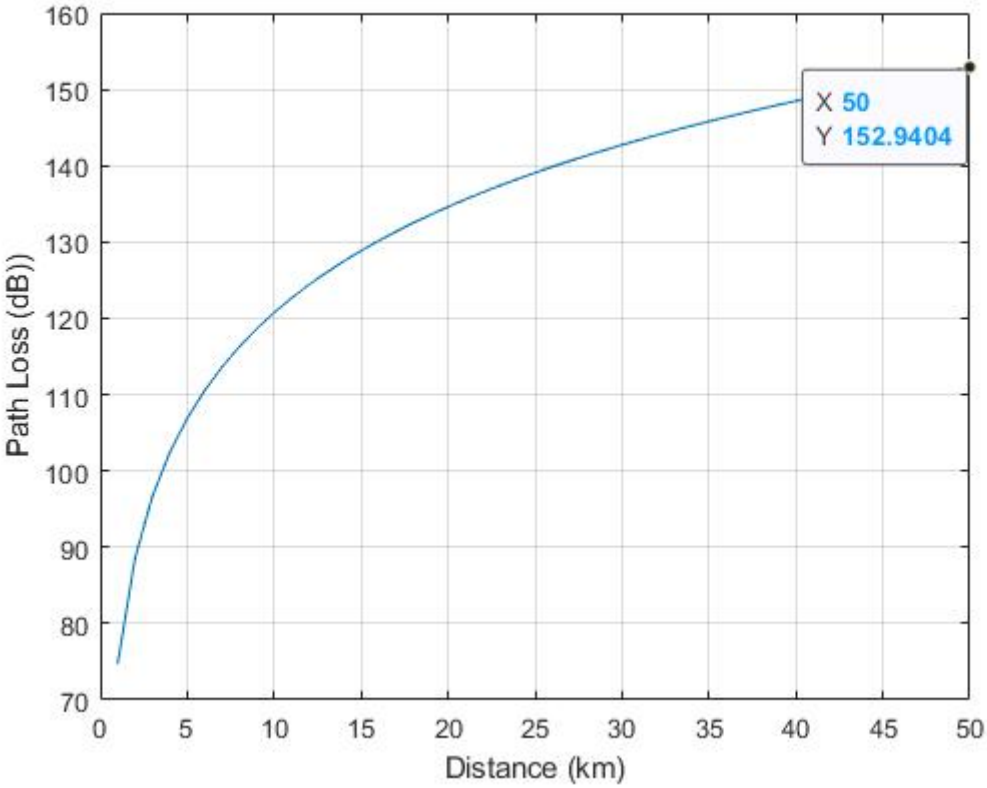

Figure 17. The path loss calculation for 50 km distance.

To visualize the effect of distance, the results of this simulation clearly indicate that the path loss increases with increasing the distance. Using 700 MHz frequency and 0 to 50 km distance, the path loss calculation over distance is shown in Figure 17. After calculating the path loss, the output results illustrates the total path loss of 153 dB for 50 km distance.

5.5 Signal-to-noise ratio

The SNR calculation over different distance values is shown in Figure 18. While the transmission power for each node is set and use the value of ideal propagation model for remote area environment. The link-level simulator allows only limited parameters of propagation model. The SNR is calculated using the Equation (22).

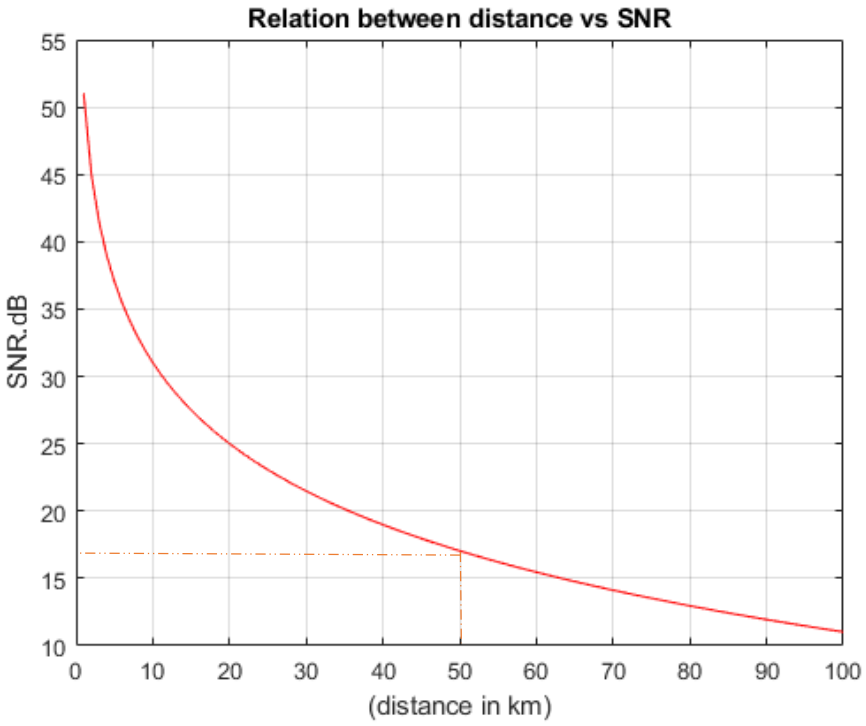

Figure 18. SNR vs. distance for different path loss values.

The relationship of SNR is analysed over different values of distance. It can be observed from the results that with this set of 50 km distance of a remote area communication which achieves the SNR level of 17 dB.

5.6 Performance analysis between two remote area users

The throughput is determined as the number of successful bits transmitted and it is typically measured in bits per second. The remote area scenario is assumed for two users, and this remote area scenario is created in the Vienna 5G link-level simulator. The link-level simulator is used to find a specific comparison output between waveform candidate and channel coding scheme for remote area communication. The above finding shows that polar code has the best performance over LDPC channel coding schemes. Similarly, the GFDM shows better OOB emission and BER output compared with OFDM waveform using 'Pedestrian A' channel. For remote area scenarios, GFDM is used as a waveform together with polar code for UE1, and LDPC code is used for UE2 as a channel coding scheme for evaluating the throughput performance between two remote area users. Table 4 shows the other different simulation input parameters for performance analyses among two remote area users.

5.6.1 Throughput performance of channel coding

The simulated throughput for SISO transmission systems with regard to SNR is discussed here. Figure 19 shows the mean throughput vs. mean SNR in 'Pedestrian A' channel for two remote area users with different channel coding schemes (polar code & LDPC code) using GFDM

technique for both case. Here, the throughput performance is addressed with 64QAM for both remote area users.

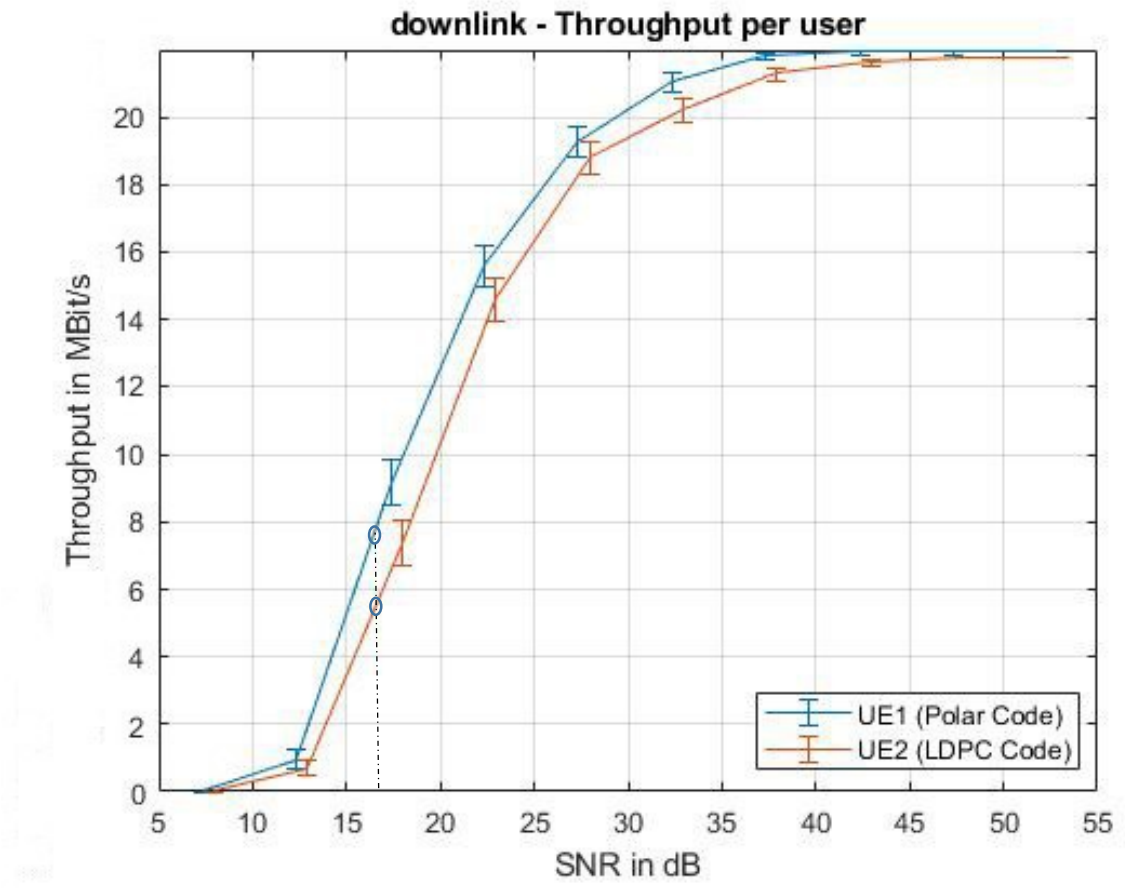

Figure 19. Throughput curves using 64QAM modulation in 'Pedestrian A' channel for different remote area users (UE1= polar code, UE2 = LDPC code).

It can be seen that the throughput is almost zero for both remote area users for low SNR 5 dB value, respectively, with 64QAM. The user's throughput improves with high SNR. In this situation, the UE1 gets with polar code the almost highest cell throughput 22 Mbps for the SNR value of 40 dB. Using LDPC code for UE2 gets the maximum throughput almost 22 Mbps after 45 dB of SNR. In case of remote area scenario for 50 km distance, the remote area users get maximum throughput of around 7 Mbps (polar code) and around 5 Mbps (LDPC code), respectively, for 17 dB SNR value. It could be seen that throughput performance of polar code shows the better performance also for other SNR values.

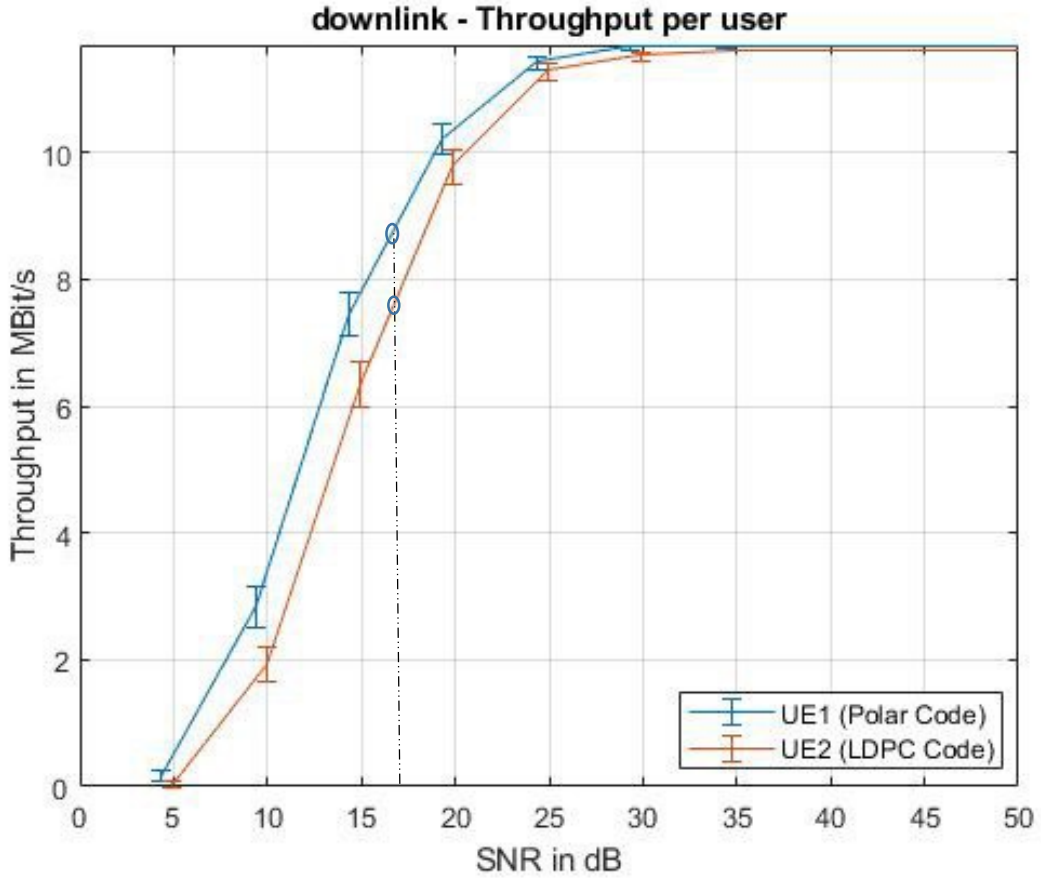

Figure 20. Throughput curves using 16QAM modulation in 'Pedestrian A' channel for different remote area users (UE1= polar code, UE2 = LDPC code).

Figure 20 shows the derived throughput performance using the 16QAM modulation. Here, the remote area users get maximum throughput of around 9 Mbps (polar code) and around 7 Mbps (LDPC code), respectively, for 50 km (17 dB) distance. For 16QAM, the UE1 gets the highest throughput performance at the SNR 30 dB, and UE2 gets the maximum throughput after 35 dB of SNR value, which is 5 dB higher than that of polar code. When comparing the results of Figure 19 and Figure 20, 64QAM gives the better throughput than 16QAM for higher SNR value. Overall, for a 50 km distance, 16QAM gives better throughput performance for low SNR along with polar code.

5.6.2 Throughput performance of waveforms

The throughput analysis has been performed for 64QAM and 16QAM modulation with 72 sub carriers using polar code for both user. The polar code is used as a coding scheme together with OFDM for UE1, and GFDM is used for UE2 as a waveform for evaluating the throughput performance between two waveforms. In this work, the throughput analysis is performed for the 'Pedestrian A' and the results are captured in the Figure 21 and Figure 22.

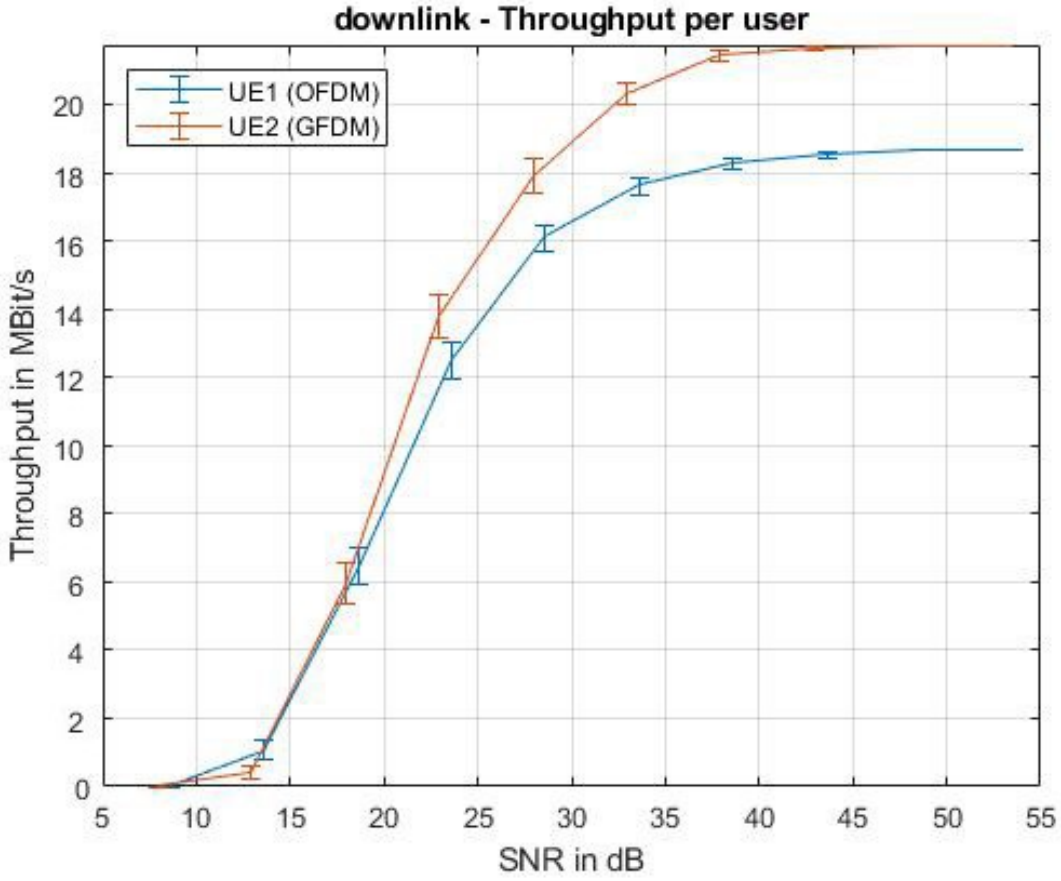

Figure 21. Throughput performance curves using 64QAM modulation in 'Pedestrian A' channel for waveforms (UE1= OFDM, UE2 = GFDM).

Figure 21 shows the comparison of the throughput performance of remote area users for 64QAM using OFDM (UE1) and GFDM (UE2) waveforms. From Figure 21, it is observed for 64QAM case the maximum throughput of 22 Mbps is attained by GFDM, whereas the OFDM attains maximum throughput of 19 Mbps. One more key observation from Figure 21 is the throughput stable at higher SNR values for the OFDM. At 17 dB SNR, it can be observed that throughput performance for both waveforms are very similar. The GFDM exhibit a significant improvement in the throughput with respect to OFDM for high SNR value.

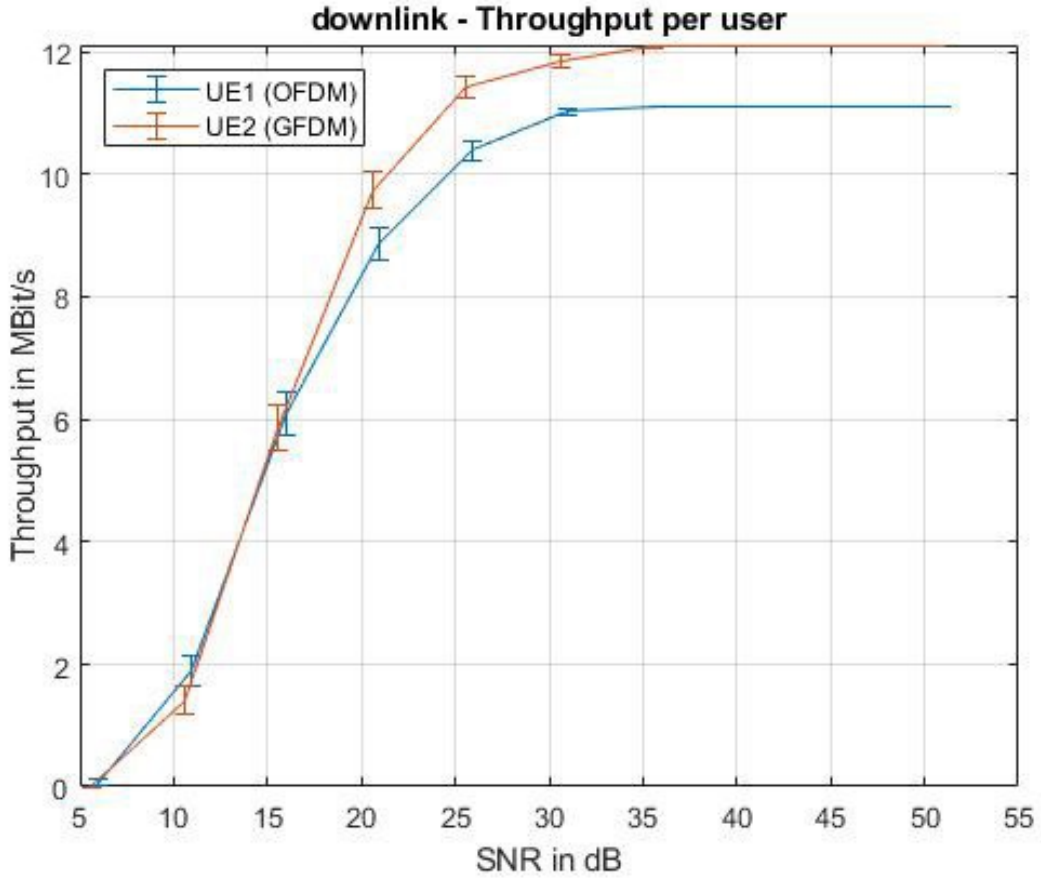

Figure 22. Throughput performance curves using 16QAM modulation in 'Pedestrian A' channel for waveforms (UE1= OFDM, UE2 = GFDM).

From Figure 22, in case of 16QAM, GFDM based UE2 achieved a maximum throughput of 12 Mbps for 35 dB SNR value and the OFDM comes with a closer value of 11 Mbps maximum throughput for same SNR Value. It can be concluded that the GFDM can perform better than OFDM based UE1. Similarly, the key observation from Figure 22 that the throughput stable at higher SNR values for the OFDM of case of 16QAM. As the order of the QAM increases, the distance in the constellation diagram between the various points decreases, and there is a significantly higher possibility that data errors may be introduced. In order to use QAM formats for high order, it is necessary to have a very high SNR else there will be present data errors. When the SNR gets worse, then it is necessary to increase the power level or reduced the order of QAM whether the data error rate is to be sustained.

6 CONCLUSIONS

This work evaluated 5G in a remote area scenario using two main techniques, such as waveforms and channel coding schemes. A generic comparison between waveforms and channel coding schemes is made. The positive and negative effects on various parameters of the waveforms and channel coding schemes have been confirmed by simulation. The SNR, FER, BER, and throughput issues have been studied. In this work, performance of BER, FER and throughput are simulated to determine the appropriate waveforms and channel coding schemes for remote area communication.

From the findings, this study infers by stating that in contrast with OFDM techniques studied in this work, GFDM is the best choice for remote area communication over 'Pedestrian A' power delay profiles. GFDM indicates better BER and spectral efficiency performance with comparison to OFDM waveform. The GFDM waveform is still to be researched and developed. The OFDM waveform should always be taken into consideration, as GFDM is much more complicated than OFDM. However, it is required in order to determine to assess the benefits and drawbacks of OFDM and GFDM as their implementation for 5G applications is advancing.

As far as channel coding is concerned, the analysis of the LDPC and polar coding schemes of the 5G mobile communication system for medium-length message transmission in the remote area was considered on an AWGN channel with a code rate of 1/3. The polar coding scheme seems to be the best possible channel code for medium-length message data transfer in remote areas based on the analysis of LDPC channel coding scheme.

The different remote area user's throughput performance have been evaluated for 50 km distance in terms of 16QAM and 64QAM modulation techniques. For 16QAM, the remote area UE1 (polar code) gets the maximum throughput performance for 17dB SNR value compare to the 64QAM modulation technique. Further, the remote area UE2 (GFDM) gets the maximum throughput performance for 16QAM compare to the OFDM technique. Based on the throughput performance of different remote area users, the polar code shows the better throughput performance for both modulation techniques compare to the LDPC code for remote area communication of 50 km distance. Similarly, the throughput performance of GFDM and OFDM waveforms for the remote area users, where the results demonstrate that GFDM waveform is quite well perform compare the OFDM for both modulation techniques (16QAM and 64QAM).

.

7 SUMMARY

To evolve mobile communications from LTE to 5G and beyond, the link-level simulation is a useful tool that enables advanced PHY methods to be researched and developed. Throughout this thesis, the Vienna 5G link-level simulator was introduced, which supports 5G research and improves reproducibility for the researchers. In compliance with existing connectivity requirements as 5G NR, this simulator supports generic simulation scenarios and parameter configuration. This study focused on the simulation parameters of 5G physical layer as well as remote area scenario for mobile communication. The key specifications of the physical layer and the most common mobile communication situations in the remote area were the main subject of this analysis.

In this study, an initial performance analysis of 5G downlink is performed using a Vienna 5G link-level simulation platform built in compliance with the 3GPP specified 5G NR specifications. Firstly, a theoretical introduction was performed on 5G NR in general based on recent works and 3GPP information (specifications, articles, overviews). The transmitter and receiver functions of remote area scenario are specified in this work.

This work focused on OFDM and GFDM waveforms, including power spectral density and bit error rate efficiency of waveforms. The output results present the transmission-side OOB emissions performance of OFDM and GFDM. The performance of OOB emission-quality is shown in scenario setup by OFDM and GFDM.

The evaluation of different channel coding schemes is mainly based on satisfying user requirements of remote area communication. The analysis of the LDPC and polar coding schemes for the 5G mobile communication system for medium length message transmission (1024 bits) in remote area communication were considered on an AWGN channel with BPSK modulation of the code rate 1/3. The assessment of the results illustrates that the polar code can be the better channel coding scheme in terms of BER and FER for remote area communication.

Based on the results, the overall performance evaluates the use of polar code and GFDM techniques for the remote area users. The output results demonstrate that polar code and GFDM techniques are quite well suited for remote area communication. In the SISO system, different remote area user's performance have been simulated and analysed with respect to 16QAM and 64QAM, where polar code and GFDM seems to have a better impact on transmission than the LDPC code and OFDM, respectably.

8 REFERENCES

[1] Martin Sauter. From GSM to LTE-Advanced Pro and 5G: an introduction to Mobile Networks and Mobile broadband. Feb. 2021, 624 p. ISBN 11-1971467-2.

[2] Ali A. Zaidi, Robert B., Mattias A., Sebastian F., Vicent M., Zhao W., Designing for the future: the 5G NR physical layer, Ericsson Technology Review, Jul. 2017.

[3] 3GPP TR 38.913. 3rd generation partnership project; 5G; Study on scenarios and requirements for next generation access technologies (release 15), V14.2.0, 2017.

[4] 3GPP TS 22.261, 3rd generation partnership project: technical specification group services and system aspects; service requirements for the 5G systems; stage 1; (release 16), V16.2.0, 2017.

[5] Stefan Rommer. 5G Core Networks: Powering Digitalization. Nov. 2019, 496 p. ISBN 978-0081030097.

[6] Ericsson. 5G systems, White Paper, 2017.

[7] 5G Americas Whitepaper, 5G Spectrum Vision, Feb, 2019.

[8] Ericsson. Traffic and market data report: On the pulse of the networked society, White Paper, 2014.

[9] Dahlman, E., Mildh, G., Parkvall, S., Peisa, J., Sachs, J., Selen, Y., and Skold, J., 5G wireless access: requirements and realization, IEEE Communications Magazine, vol. 52, no. 12, pp. 42–47, Dec. 2014.

[10] Osseiran, A., Boccardi, F., Braun, V., Kusume, K., Marsch, P., Maternia, M., Queseth, O., Schellmann, M., Schotten, H., Taoka, H., Scenarios for 5G mobile and wireless communications: the vision of the metis project, IEEE Communications Magazine, vol. 52, no. 5, pp. 26–35, 2014.

[11] 6G channel, 6G white paper on connectivity for remote areas. Apr, 2020; Available at: https://arxiv.org/ftp/arxiv/papers/2004/2004.14699.pdf.

[12] Stefan Pratschner, Vienna 5G LL simulator user manual, Feb. 2019. Available at: https://www.nt.tuwien.ac.at/wp-content/uploads/2018/06/5GLL userManual.pdf.

[13] 5G-RANGE, Remote Area Access Network for the 5th Generation, D2.1 Application and requirements report, Apr, 2019. Available at: http://5g-range.eu/wp-content/uploads/2018/04/5GRange_D2.1_Application_Requirement_Report_v1.pdf.

[14] 5G-RANGE, Remote Area Access Network for the 5th Generation, Deliverable 3.1 Physical layer of the 5G-RANGE-Part I, Apr, 2018.

[15] ETSI. Digital cellular telecommunications system (phase2+), Universal Mobile Telecommunications System (UMTS), “124008:", May 2019.

[16] Ali Zaidi. 5G Physical Layer, Principles, Models and Technology Components. Jan. 2018, 322 p. ISBN 01-2814578-1.

[17] GSMA. 5G Spectrum, GSMA Public Policy Position, Mar, 2020. Available at: https://www.gsma.com/spectrum/wp-content/uploads/2020/03/5G-Spectrum-Positions.pdf.

[18] GSMA. The 5g guide a reference for operators, Apr, 2019. Available at: https://www.gsma.com/wp-content/uploads/2019/04/The-5G Guide_GSMA_2019_04_29_compressed.pdf.

[19] G. Liu, Y. Huang, Z. Chen, L. Liu, Q. Wang and N. Li, 5G Deployment: Standalone vs. Non-Standalone from the Operator Perspective, in IEEE Communications Magazine, vol. 58, no. 11, pp. 83-89, November 2020, doi: 10.1109/MCOM.001.2000230.

[20] 3GPP TS 38.211, 3rd generation partnership project: physical channels and modulation (release 16), V16.4.0, 2020.

[21] SG05. Draft new report itu-r m.[imt-2020. tech perf req]-minimum requirements related to technical performance for imt-2020 radio interface (s), 2017. Available at: https://www.itu.int/md/R15-SG05-C-0040/en.

[22] Mousavi, H., Iraj S., Amiri., Mostafavi., M.A., LTE physical layer: Performance analysis and evaluation, applied commuting and Informatics, Sep. 2017.

[23] Islam N., Rashid M., Pasandideh F., Ray B., Moore S., Kadel R. (2021). A Review of Applications and Communication Technologies for Internet of Things (IoT) and Unmanned Aerial Vehicle (UAV) Based Sustainable Smart Farming. Sustainability. 13. 1821. 10.3390/su13041821.

[24] Lihua Y., Longxiang Y., Yan L., Iterative Channel Estimation for MIMO-OFDM system in Fast Time Varying Channels, KSII Transactions of Internet and Information Systems, Vol. 10, No. 9, Sept. 2016.

[25] Aida Z., and Ridha B., A Full Performance Analysis of Channel Estimation Methods for Time Varying OFDM Systems, International Journal of Mobile Network Communication & Telematics, Vol.1, No.2, Dec, 2011.

[26] 3rd Generation Partnership Project (3GPP): Technical Specification Group Radio Access Network; Study on New Radio (NR) access techology. TR 38.912, 3GPP, V15.0.0, June 2017.

[27] 3GPP, Technical specification (TS) 36.212 - E-UTRA; Multiplexing and channel coding, V15.2.1. Jul. 2018.

[28] Pathwave, 5G Waveform Evaluation, for mmWave Communication Using System Vue. Mar, 2019. Available at: https://www.keysight.com/fi/en/assets/7018-05956/application-notes/5992-2647.pdf.

[29] HAL. Waveform contenders for 5G: Description, analysis and comparison, Physical Communication, Jul, 2019. Available at: https://hal-cea.archives-ouvertes.fr/cea-01848639/file/2017_Elsvier_Waveform_contenders_for_5G_Description_Analysis_and_Comparison.pdf.

[30] Mahmoud, H. A., Yucek, T., Arslan, H., OFDM for cognitive radio: merits and challenges, IEEE Wireless Communications, vol. 16, no. 2, pp. 6-15, Apr, 2009.

[31] Bastian B., Michele S., Christoph S., Falko D., Towards an Open Source IEEE 802.11p Stack: A Full SDR-based Transceiver in GNU Radio, in Proc. of 5th IEEE Vehicular Networking Conference (VNC 2013), Boston, MA, pp. 143-149, Dec. 2013.

[32] Fuxjager, P., Cotantini, A., Valerio, D., Castiglione, P., Zacheo, G., Zemen, T., Ricciato, F., IEEE 802.11p Transmission Using GNU Radio, in Proc. of 6th Karlsruhe Workshop on Software Radios, Karlsruhe, Germany, Mar, 2010.

[33] Mendes, L., Michailow, N., Matthé, M., Gaspar, I., Zhang, D. Fettweis, G., GFDM: Providing flexibility for the 5G physical layer, in Opportunities in 5G Networks: A Research and Development Perspective, CRC Press, 2016.

[34] Juliano F., Henry R., Arturo G., Ahmad N., Maximilian M., Dan Z., Luciano M., Gerhard F., GFDM Frame Design For 5G Application Scenarios, Journal of Communication and Information Systems, vol. 32, no.1, 2017.

[35] Muhammad S., Inam Ullah K., Nazia A., Comparison of GFDM and OFDM with respect of SER, PSD and PAPR, et al, International journal of Mechanical Engineering & Computer Applications (IJMCA), Vol. 4, No. 6, Nov –Dec, 2016.

[36] Michailow N., Matthe M., Gaspar I., Caldevilla A., Mendes L., Festag A., Fettweis G., Generalized Frequency Division Multiplexing for 5th Generation Cellular Networks, IEEE Transactions on Communications, vol. 62, no. 9, pp. 3045–3061, Sept 2014, doi:10.1109/TCOMM.2014.2345566.

[37] Arikan, E. Channel polarization: A method for constructing capacity-achieving codes for symmetric binary-input memoryless channels. IEEE Transactions on Information Theory, 55(7), 3051–3073, 2009.

[38] Zhang, H., Li, R., Wang, J., Dai, S., Zhang, G., Chen, Y., Luo, H., Wang, J., Parity-check polar coding for 5G and beyond, in: IEEE Int. Conf. Commun. (ICC), Jan, 2018.

[39] Tal, I., & Vardy, A. List decoding of polar codes. IEEE Transactions on Information Theory, 61(5), 2213–2226, 2015.

[40] Niu, K., & Chen, K. CRC-aided decoding of polar codes. IEEE Communications Letters, 16(10), 1668–1671, 2012.

[41] Tahir, B., Schwarz, S., and Rupp, M., BER comparison between convolutional, turbo, LDPC, and polar codes, in 24th International Conference on Telecommunications (ICT), May 2017, pp. 1–7.

[42] 3GPP TS 36.201. 3rd generation partnership project; technical specification group radio access network; evolved universal terrestrial radio access (e-utra); lte physical layer general description (release 8). V8.3.0. Aprl. 2009.

[43] Zahraa R., and Mayoof H., Channel Coding Scheme for 5G Mobile Communication System for Short Length Message Transmission, Wireless Personal Communications 106:377–400*,* 2011, Feb, 2019.

[44] Stefan P., Bashar T., Versatile Mobile Communications Simulation: The Vienna 5G Link Level Simulator; Jan. 2020. Available at: https://arxiv.org/pdf/1806.03929.pdf.

[45] 3GPP (2018) Study on channel model for frequencies from 0.5 to 100 GHz (Release 15). TR 38.901, V15.0.0, Jun, 2018.

[46] William H. Principles of communication systems simulation with wireless applications. Upper Saddle River: Prentice Hall, 2003, 778 p. ISBN 01-3494790-8.

[47] International Telecommunication Union Guidelines for evaluation of radio transmission technologies for IMT-2000. Recommendation ITU-R M.1225, 1997. Available at: https://www.itu.int/oth/R0A0E00000C/en.

[48] Niranjane, V. B., and Bhoyar, D. B., Performance analysis of different channel estimation techniques, in International Conference on Recent Trends in Information Technology (ICRTIT)*,* 2011, pp. 74–78.

[49] Mitić D., Lebl A., Markov Z. (2012). Calculating the required number of bits in the function of confidence level and error probability estimation. Serbian Journal of Electrical Engineering. 9. 361-375. 10.2298/SJEE1203361M.

[50] Digital signal processing, Frame error rate definition. Jan. 2021. Available at: https://dsp.stackexchange.com/questions/58035/what-is-the-difference-between-frame-error-rate-fer-and-symbol-error-rate-ser.

9 APPENDICES

Appendix 1 Parameter file for the remote area scenario.

```
%% Topology

scStr.topology.nodes                        = ['BS1,BS2,UE1,UE2'];
scStr.topology.primaryLinks                 = ['BS1:UE1,' ...
                                               'BS2:UE2' ...
                                               ];
scStr.topology.interferenceGeneration       = 'Automatic';
scStr.topology.attenuation                  = 30;
scStr.topology.interferingLinks             = [ ];

%% General Simulation Parameters

scStr.simulation.simulateDownlink           = true;
scStr.simulation.simulateUplink             = false;
scStr.simulation.simulateD2D                = false;
scStr.simulation.plotResultsFor             = [1];
scStr.simulation.plotOverSNR                = true;
scStr.simulation.saveData                   = false;
scStr.simulation.sweepParam                 = {'simulation.pathloss'};
scStr.simulation.sweepValue                 = linspace(150,90,6);
scStr.simulation.applySweepingTo            = [1];
scStr.simulation.nFrames                    = 1000;

%% Physical Transmission Parameters

scStr.simulation.centerFrequency            = 7e8;

scStr.simulation.txPowerBaseStation         = [53];
scStr.simulation.txPowerUser                = [53,53];
scStr.simulation.nAntennasBaseStation       = [2];
scStr.simulation.nAntennasUser              = [1];
scStr.simulation.userVelocity               = [130];
scStr.simulation.pathloss                   = [153];
scStr.simulation.downlinkNonlinearity       = false;
scStr.simulation.amplifierOBO               = [1];
scStr.simulation.smoothnessFactor           = [3];

%% Channel Parameters

scStr.channel.dopplerModel                  = 'Discrete-Jakes';
scStr.channel.timeCorrelation               = false;
scStr.channel.spatialCorrelation            = 'none';
scStr.channel.nPaths                        = 50;
scStr.channel.powerDelayProfile             = 'PedestrianA';
scStr.channel.K                             = 0;
scStr.channel.delta                         = 1;
```

```
%% Channel Estimation and Equalization Parameters

scStr.simulation.channelEstimationMethod    = 'Approximate-Perfect';
scStr.simulation.noisePowerEstimation       = false;
scStr.simulation.pilotPattern               = 'LTE Downlink';
scStr.simulation.equalizerType              = 'One-Tap';
scStr.simulation.receiverTypeMIMO           = 'ZF';

%% MIMO Parameters
% Layer mapping

scStr.layerMapping.mode                     = '5G';
scStr.layerMapping.table.Uplink             = {1;2;[1,2]};
scStr.layerMapping.table.Downlink           = {1;2;[1,2]};
scStr.modulation.transmissionMode           = 'custom';
scStr.modulation.delayDiversity             = 1;

%% Feedback Parameters
scStr.feedback.delay                        = 0;
scStr.feedback.averager.Type                = 'miesm';
scStr.modulation.cqiTable                   = 0;
scStr.feedback.enable                       = false;
scStr.feedback.pmi                          = false;
scStr.feedback.ri                           = false;
scStr.feedback.cqi                          = true;
scStr.modulation.nStreams                   = [1, 1];
scStr.modulation.precodingMatrix{1}         = 1/sqrt(2)*ones(2,1);
scStr.modulation.precodingMatrix{2}         = 1/sqrt(2)*ones(2,1);
scStr.modulation.mcs                        = [8,8];

%% Modulation Parameters
% Waveform

scStr.modulation.waveform                   = {'GFDM'};
scStr.modulation.prototypeFilter            = 'PHYDYAS-OQAM';
scStr.modulation.nSubcarriersPerSubband     = [12];
scStr.modulation.numerOfSubcarriers         = [72,72];
scStr.modulation.subcarrierSpacing          = [15e3,15e3];
scStr.modulation.nSymbolsTotal              = [15,15];
scStr.modulation.nGuardSymbols              = [2,1];
scStr.modulation.samplingRate               = 'Automatic';

%% Channel Coding Parameters

scStr.coding.code                           = {'Turbo', 'Polar'};
scStr.coding.decoding                       = {'MAX-Log-MAP',...
                                               'CRC-List-SC'};
scStr.coding.decodingIterations             = [8,8];

%% Schedule
% static schedule per base station

scStr.schedule.fixedScheduleDL{1}           = ['UE1:72'];
scStr.schedule.fixedScheduleDL{2}           = ['UE2:72'];
scStr.schedule.fixedScheduleUL{1}           = ['UE1:72,none:72'];
scStr.schedule.fixedScheduleUL{2}           = ['UE2:72,none:72'];
```